university of groningen / faculty of science and engineering

The effect of Mg concentration on the microstructure, mechanical properties and corrosion resistance of physical vapor deposited ZnMg coatings

IEM Bachelor Thesis

Geeske Ridder

S3425339 / PTL 36

Prof. dr. Y. Pei (1st supervisor)

Dr. ir. A. A. Geertsema (2nd supervisor)

Dr. S. Sabooni (daily supervisor)

Abstract

In this research, physical vapor deposition was employed to deposit single layer pure Zn and bi-layered ZnMg-Zn coatings onto the steel substrate. The effect of Mg concentration was then investigated on the microstructure, mechanical properties and corrosion resistance of the coatings. . It was found that the phase content of the ZnMg layer changes with increased Mg concentration from the ductile pure Zn phase to brittle intermetallic Mg_2Zn_{11} and $MgZn_2$ phases. Accordingly, the hardness and elastic modulus, and thus the coatings resistance to plastic deformation, increase with increased Mg concentration. It was also shown that the adhesion strength of the coatings at the ZnMg/Zn interface decreases with increasing Mg concentration. Lastly, the corrosion resistance of the coating was evaluated. Physical Vapor Deposition (PVD) was shown to be favorable in the case of coatings corrosion resistance over the currently used Hot Dip Galvanizing (HDG). Besides this, ZnMg coatings showed great corrosion resistance compared to commercially applied coatings due to the formation of a thin and dense layer of corrosion products.

Table of Contents

1. Literature Review

In the first part of this report a literature review will be carried out as preliminary research, with which a more thorough understanding of the subject is gained. Several aspects of the subject will be addressed in detail. Starting off with the incentive of applying a coating to steel: corrosion. After which a more detailed explanation will be given of what coatings are commonly used, what improvements were made on these coatings in the past few years and why Mg in specific is a beneficial alloying element for the Zn coating. Then several techniques with which the coating can be applied to the steel substrate are discussed. Lastly, issues arising by the Mg addition, which is mainly concern adhesion strength, and how this can be measured and possibly solved will be addressed. The goal of this literature review is to gain a thorough understanding of the material, so that valid conclusions can be drawn from the data analysis which will be done thereafter.

1.1: Corrosion of steel structures

First of all, a more detailed explanation has to be given as to why it is necessary to coat steel products. When metals, such as steel, are exposed to the atmosphere, reactions start to occur between the metal product and its surroundings. The (electro)chemical reactions that take place between the metal and the environment are more commonly referred to as corrosion [1]. Corrosion has a negative effect on the steel product, as it generates degradation of the surface quality of the product.

Looking specifically into the case of steel, it was found that most steel structures, such as those used in the automotive industry, are often exposed to several corrosive elements, including water, salt-laden air and rain and other chemicals that appear in the atmosphere [1]. When the steel structure comes into contact with one of these corrosive elements, the iron, which is the main element in steel, will form rust (Fe_2O_3) in combination with the oxygen present in the atmosphere. The process in which this rust is formed is called oxidation, which is an electrochemical process as there is an electrical current present which induces the reaction. For the reaction to occur several components have to be present, which are all part of the corrosion cell. In this cell the iron at the anodic side oxidases, releasing electrons, which travel towards the cathodic

side, where they react with oxygen. This oxygen then in turn reacts with the oxidized iron from which rust is formed as seen in fig. 1.1 [1].

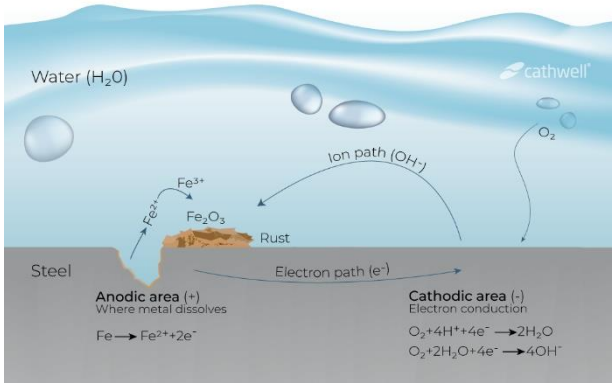

Fig. 1.1: Schematic overview of a corrosion cell [2]

As the rust formation has a negative effect on the quality of steel and its process occurs naturally when the right components are present, a preventive measure or solution must be found to resolve this problem. As stated before, a possible solution to this problem is to apply a protective coating to the steel structure, which increases its corrosion resistance, in order to maintain its initial quality and structure. In the next section a more thorough explanation will be given on what coatings are commonly used on steel and what improvements can be made to these.

1.2: Pure Zn coatings

The protection of steel structures is thus ensured by the addition of a coating on top of the steel substrate. This coating can be made of many types of elements, but the most commonly used and commercially applied are zinc (Zn) coatings [3]. Zn coatings give galvanic protection to the substrate, which means that it sacrificially corrodes over time. This is because the nobility of Zn is lower than that of the iron (Fe) present in the steel at regular conditions, and therefore it will corrode first, even if there are gaps present in the Zn coating [3]. Before a better insight can be gained of how this Zn coating protects the steel substrate and what corrosion mechanisms take place, it is essential to first understand how Zn reacts with Fe to form the coating on the steel substrate.

1.2.1: Fe-Zn phases and layer formation

When the Fe present in the steel substrate comes into contact with Zn, it will react and different phases will be formed. This phase formation is summed up in a phase diagram, which is shown in fig. 1.2a. A zoomed in overview of the Zn rich corner, which will give a better overview of what phases will be formed in the Zn coating is given in fig. 1.2b. Exactly what phases will be present to what extend depends on the

temperature at which the Zn and Fe will react with each other, which depends on the type of process used for the application of the coating. Up until now, the most commonly used methods for this are hot dip galvanizing (HDG), thermal spraying and electrodeposition [3]. For determining the phases present in the coating the temperature of the HDG method (450 – 490 ^{0}C) will be used. From the phase diagram it can then be seen that the following phases will be present: Γ (Fe_3Zn_{10}), Γ_1 (Fe_5Zn_{21}), δ ($FeZn_{10}$), ζ ($FeZn_{13}$).

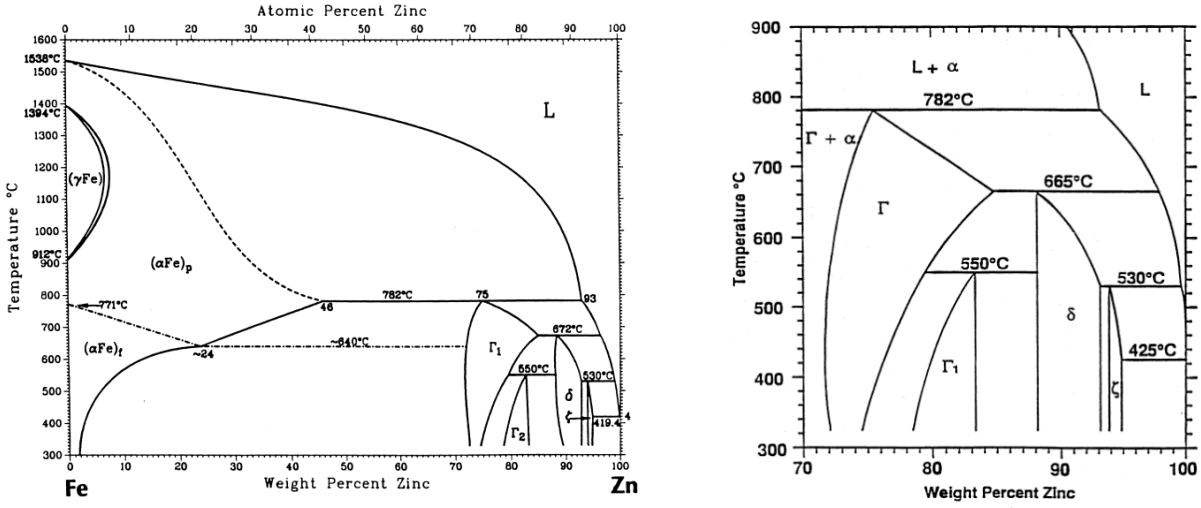

Fig. 1.2a: Full phase diagram of Fe-Zn; Fig. 1.2b: Zn rich corner of Fe-Zn phase diagram [4]

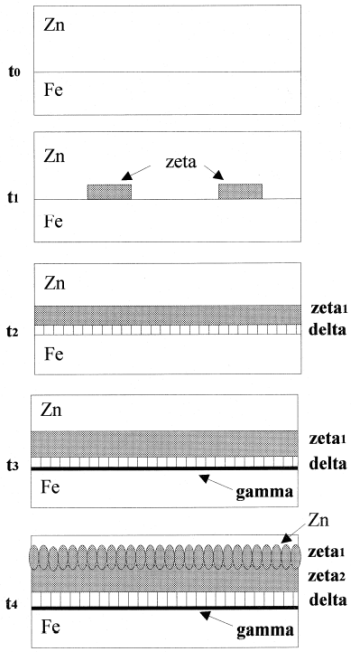

Fig. 1.3: layer formation of the different Fe-Zn phases [5]

Fig. 1.3 shows the formation of these different phases. First off, the Zn rich zeta phase is formed, where after the delta phase forms at the interface of the zeta phase and steel substrate. Thirdly, the gamma phase will start to form at the interface of the delta phase and steel substrate. Lastly, the zeta phase splits up into two phases [5].

1.2.2: Corrosion mechanisms of pure Zn

After understanding how the Zn coating is formed on the steel substrate, a more thorough explanation can be given on how this applied coating actually protects the steel. The Zn layer protects the steel substrate in two ways, through barrier protection and galvanic protection [3]. Barrier protection simply means that the coating isolates the steel substrate from the surrounding atmosphere and therefore makes it impossible for the steel to corrode, like explained in the first section. Instead of the steel substrate corroding, the Zn layer on top will corrode. Although the Zn coating will slowly vanish, its corrosion rate is much lower (10-30 times) than that of the steel substrate, and will therefore guarantee a longer period of protection [6].

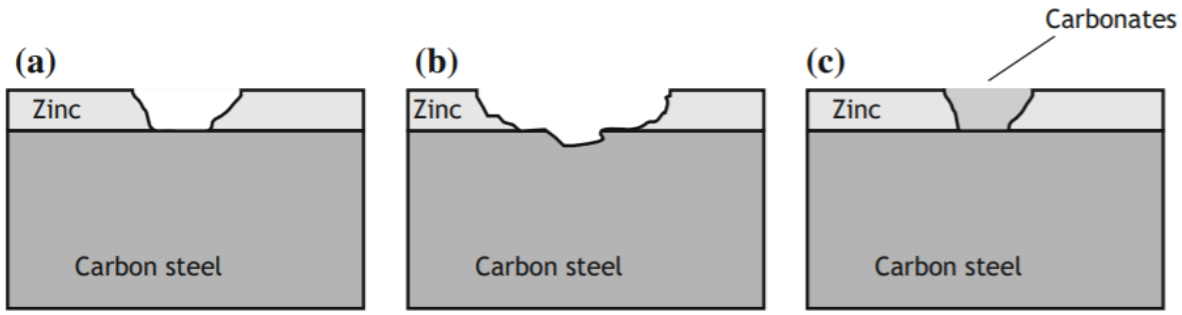

Fig. 1.4: Galvanic protection of the Zn coating under different circumstances (Pedeferri, 2019)

Besides barrier protection, the Zn coating also offers galvanic protection. This type of protection is present at the defective spots in the coating. For example, when there is a small crack or dent in the protective coating, which means that some of the steel substrate will be exposed to the surrounding atmosphere, the adjacent Zn will still protect the steel substrate. This is due to the low nobility of Zn compared to that of the Fe in steel, which means that Zn is more electronegative and thus more reactive. Because of this, the Zn will sacrifice itself and therefore corrode, instead of letting the Fe react with elements in the surrounding and letting the steel substrate corrode [6]. Unfortunately, this type of protection is not always given, for example when gaps or scratches in the coating are too big the steel could possibly start corroding, but this is dependent on the surrounding atmosphere. In fig. 1.4a it can be seen that the galvanic protection works properly if the defect is not too large, and that therefore the Zn on the sides of the defects only start to slowly corrode. Opposing to this, in fig. 1.4b, it is shown

that when the defect size increases, the steel is not fully protected anymore. In this case, the steel will start to corrode in the middle of the defect, because at that specific spot the Zn coating is too far away. This means that at that place the electronegativity of the Zn coating is not sufficient enough anymore to draw the elements with which the corrosion reactions take place towards the coating instead of the steel substrate, and thus the substrate will corrode. In fig. 1.4c it is shown how the formation of carbonates can provide a sealing effect for the defects in the coating [6]. How this sealing effect is formed will be explained in the following subsection.

1.2.3: Chemical reactions occurring in the corrosion mechanism of pure Zn

When galvanized steel, a steel protected with a Zn coating, comes into contact with the surrounding atmosphere, several reactions will take place, depending on the types of elements present in that atmosphere. For example, when the galvanized steel is exposed to an atmosphere in which both oxygen and water are present, aqueous

$$Zn(s) \rightarrow Zn^{2+} + 2e^{-} \tag{1.1}$$

corrosion will take place using the following reactions [7]:

First of all, the Zn present at the anodic sites, the sites where the Zn coating has to sacrifice itself for the steel substrate, will oxidase. This reaction needs to be balanced, which is done by the reduction of dissolved oxygen:

$$\frac{1}{2}O_2 + H_2O + 2e^{-} \rightarrow 2OH^{-} \tag{1.2}$$

The cation and anion formed in reactions 1 and 2 will then react with each other, which consequentially created zinc oxide (or zinc hydroxide). The full reaction is given by the following:

$$Zn(s) + \frac{1}{2}O_2 + H_2O \rightarrow Zn(OH)_2(s) \rightarrow ZnO(s) + H_2O \tag{1.3}$$

If the pH of the corrosive atmosphere is high enough, the zinc oxide may even react further on following this reaction:

$$ZnO(s) + 2OH^{-} + H_2O \leftrightarrow Zn(OH)_4^{2-} \tag{1.4}$$

This reaction forms a zincate ion, which stimulates oxygen reduction by keeping the Zn surface accessible, and thus increases corrosion.

When sodium-chloride is present, which is common in most atmospheres, chloride ions can be formed, with which the formation of simonkolleite ($Zn_5(OH)_8Cl_2 \cdot H_2O$):

$$5ZnO(s) + 2Cl^- + 6H_2O \leftrightarrow Zn_5(OH)_8Cl_2 \cdot H_2O(s) + 2OH^- \quad (1.5)$$

The formation of simonkolleite can have a positively increase the corrosion resistance of the coating, as will be explained more thoroughly further on in this section, but the simonkolleite requires a very specific pH (6-8). As can be seen in (5), with the formation of simonkolleite, 2 hydroxide anions are also created. These increase alkalinity and thus decrease the stability of the simonkolleite. If these hydroxide anions are not neutralized, for example by (4), then the simonkolleite will react backwards (reverse of (5)). Once this happens, the chloride ions are released and able to react again. They will then increase the overall electrolyte conductivity, which increases the corrosion rate [7].

Another reaction which can occur on the surface of the coating is the formation of a carbonate. This will occur when a sufficient amount of carbon dioxide is present in the atmosphere. First of all, the carbon dioxide must react with the hydroxide anions to form a carbonate, after which this carbonate reacts with even more carbon dioxide to form hydrogen carbonate. This is shown in the following reactions:

$$CO_2 + 2OH^- \leftrightarrow CO_3^{2-} + H_2O \quad (1.6)$$

$$CO_2 + CO_3^{2-} + H_2O \leftrightarrow 2HCO_3^- \quad (1.7)$$

These sequential reactions decrease the pH of the surface and thus decrease the alkalinity, which is favorable for the simonkolleite. But there is also a possibility that sodium ions, which were split from the chloride ions, will react with the carbonate, which in turn increases alkalinity.

Assuming that the hydrogen carbonate forms, this last reaction can take place:

$$4ZnO(s) + 2HCO_3^- + 3H_2O \leftrightarrow Zn_4CO_3(OH)_6 \cdot H_2O(s) + CO_3^{2-} \quad (1.8)$$

In this last reaction zinc hydroxy carbonate is formed, which also helps increase the corrosion resistance. As stated before, the simonkolleite layer cannot exist if the surface of the coating is to alkaline, but this can be resolved by the formation of carbonates as seen in reaction (6) to (8). If the overall pH at the surface is brought to 6-8 the simonkolleite will remain stable and corrosion resistance will increase, as this retards the corrosion mechanism occurring between pure Zn and the atmosphere.

1.2.4: Corrosion resistance of Zn coatings in different environments

In fig. 1.5 the corrosion rate of a Zn coating is shown when exposed to different types of environments. This ranges from very low to very high corrosivity, respectively C1 till C5 [6]. As can be seen in the figure the corrosion rates do all remain constant, but they do vary a lot. This is because different elements can be present in different atmospheres. For example, in the previous section it was shown that when carbon dioxide is present, a certain carbonate can be formed which helps increase the corrosion resistance. When looking at more acidic/corrosive environments, such as polluted or marine areas, it is possible that different reactions take place, such as the formation of zinc sulphate. The products formed in these increasing corrosive environments are overall more soluble, and thus yield less protection to the Zn, enabling the corrosion rate to increase [6].

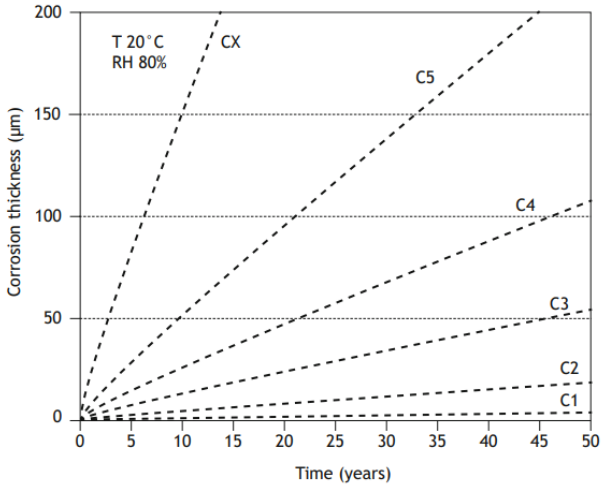

Fig. 1.5: corrosion resistance of Zn coatings in different environments [6]

1.3: Alloying of the Zn coating

This section will explore how the alloying of the Zn coating can increase its corrosion resistance, which improves the protection of steel from the environment. The most frequently studied alloying elements are aluminum, magnesium, silicon, copper tin and nickel [8]. In the three subsections down below an overview will be given of how the Zn coatings were improved over past years and what alloying elements are most beneficial.

1.3.1: Addition of aluminum

One of the first alloying elements which was added to the Zn coating to increase corrosion resistance was aluminum (Al). Many different proportions of alloying with Al have been investigated and also commercially applied. The most commonly known

and applied variants of ZnAl coatings are Galvalume (Zn-55Al) and Galfan (Zn-5Al) [8].

Galvalume was commercially developed in 1970 and contains a large amount of Al (55wt%). An extra addition of 1.5 wt% silicon (Si) is also added to the bath, which prevents an exothermal reaction (Marder, 2000). The addition of Al leads to the formation of intermetallic Fe-Zn-Al compounds at the interface of the steel substrate and the coating. This coating does not only show improved corrosion resistance, but also better adhesion to the substrate [8].

Galfan was developed in the 1980's and is thus a Zn coating with 5 wt% Al. This amount of Al alloying leads to the formation of eutectic composition consisting of a pro-eutectoid η phase, which is rich in Zn, and a eutectoid phase consisting of both η and β phases [8]. This coating was commercially developed as it showed improved corrosion resistance, about 2-3 times more protective, compared to that of pure Zn coatings [9] and also due to its good conformability. Small additions of other elements were also added to the bath to ensure wettability, which included 0.5 wt% of lanthanum, cerium and magnesium [8].

1.3.2: Addition of silicon and magnesium

As discussed earlier, the addition of Al to the Zn coating already yields better corrosion resistance and also some other preferable properties over traditional galvanized coatings. Although this addition was already quite an improvement, it was also shown that additions of small amounts of other alloying elements, such as magnesium and silicon, to the Zn-Al coatings yielded even better results. The main problem with Zn-Al coatings is that the intermetallic Al-Fe compound grow really fast and form a thick layer at the interface of the steel substrate and the coating affecting the formability of the coating [10].

So to make further improvements to the coating different alloying elements were tested. In the research of Tanaka et al. [11] it was investigated how the addition of both silicon (Si) and Mg had an effect on the surface morphology, microstructure and corrosion resistance of the coating. This was tested by comparing two coatings which were both dipped twice into a Zn bath. The first bath consisted of pure Zn and the second of Zn-6Al with or without 0.5 wt% Mg and 0.1 wt% Si. It was shown that the addition of Si and Mg yielded a more homogeneous and slower corrosion, whilst the Zn-ZnAl coating corroded faster locally.

1.3.3: Zn-Al-Mg coatings

One of the coatings that was investigated thoroughly more recently is the Zn-Al- Mg coating. This coating showed several advantages over traditional coatings. First of all,

its performance was proven to be 10-20 times better than that of galvanized coatings and 2-5 times better than that of Zn-Al coatings in salt spray tests. Also, the addition of Mg to the coating was shown to generate a “self-healing” property, with which it is meant that the dents or defects in the coating were filled up with a sort of protective layer. Thirdly, the corrosion resistance is much better due to improved microhardness. Lastly, the density of Al and Mg is lower than that of Zn, so the overall mass of the coating is lower, which is also beneficial [10].

1.4: Advantage of ZnMg coatings

Up until now, several alloying elements and combinations have been discussed, including Mg. Recent researches have shown that Mg yields very promising alloying elements for improving corrosion resistance of the steels and should therefore be further investigated. Therefore, this section will elaborate on ZnMg coatings in specific. It will first show some more results of literature regarding this particular coating, where after a more thorough understanding is gained as to why the addition of Mg generates such promising corrosion resistance.

1.4.1: Corrosion resistance improvements by addition of Mg

In the previous section the Zn-Al-Mg coatings were already discussed, which were shown to have very promising performance compared to traditional galvanized coatings and Zn-Al coatings such as Galfan and Galvalume. Recent studies have shown that the Zn-Mg coatings do not only exceed those coatings, but also many other Zn alloyed coatings concerning corrosion resistance. Therefore, Zn-Mg coatings are expected to provide the most promising possibilities in decreasing coating thickness and perhaps eliminating pre-treatment of the steel substrate, which are both strong wishes of the automotive industry [12].

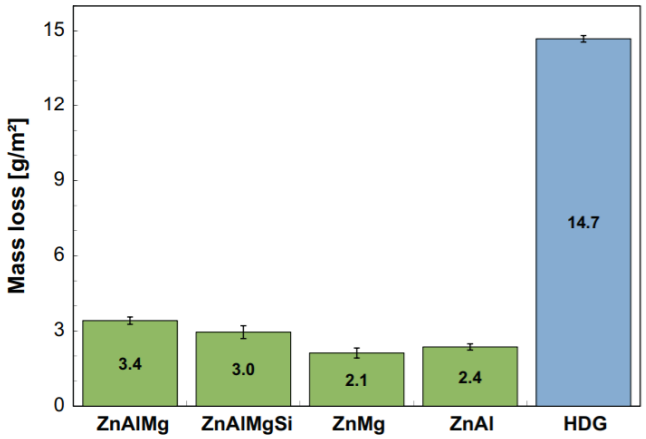

Fig. 1.6: mass loss of different Zn, Zn-Al and Zn-Al-Mg coatings describing the amount of corrosion that occurred [13]

In a research conducted by Prosek et al. [13] different alloyed Zn coatings were studied and compared, which included Zn-Al-Mg, Zn-Al-Mg-Si, Zn-Mg, Zn-Al and a traditional galvanized coating. The coatings were exposed to an environment containing Na-Cl, which was supposed to imitate atmospheric conditions. One of the parameters investigated was the mass loss of the different coatings, which indicates to what extent they are corroded. Fig. 1.6 shows an overview the mass loss of different coatings, which clearly indicates that the addition of Al and Mg as alloys in the Zn coating leads to increased corrosion resistance, but also shows that the Zn-Mg coating demonstrate best, although the difference compared to the Zn-Al coating is not that large.

Some other studies have shown even greater improvements in corrosion resistance and other parameters concerning Zn-Mg coatings, but many of the experiments of these studies were carried out in very corrosive environments which do not properly represent atmospheric conditions and therefore also yield different outcomes [13].

1.4.2: Comparison of ZnMg coatings versus pure Zn coatings

Now that the promising performance of Zn-Mg coatings compared to traditional and other alloyed coating has been discussed, a more thorough understanding has to be gained about the reason for this performance. Several studies have been performed investigating the complex corrosion mechanisms of Zn-Mg coatings, but they all propose slightly different justifications for this increased performance.

One of the main findings for coatings with high concentrations of Mg was that it showed an inversion in potential between the defects in the coating where corrosion usually occurs and the intact interface. In this inversion the potential of the intact interface would be lower than that of the corroding defect. This would inhibit the electron transfer even more and thus not make delamination of the coating possible. Although this would mean that the coating would practically be resistant to delamination, even without additional treatments, there are many dangers to it. If the inversion of potential is abolished and the normal situation returns, corrosion will occur again. This can happen at smaller not very actively corroding defects and at alkaline pH levels at defects [12].

Many studies also showed that the formation of Mg-rich oxides which formed a layer on the Zn-Mg coating, thereby inhibiting oxygen reduction was the main reason for the increased corrosion resistance. Others also stated that it was due to the formation and stabilization of the simonkolleite layer, or zinc hydroxysulfate [12].

For example, the study of Hosking et al. proposed that the good corrosion resistance was enabled by the formation of magnesium hydroxide, which precipitated at the cathodic areas of the coating lowering the pH value of the surface area of the coating. The magnesium hydroxide can then further react with CO_2 to form carbonates which

also lowered the pH. It was suggested that due to this more neutral pH on the surface area of the coating, a stable simonkolleite layer could form, as this has a very specific stability range (pH 6-8).

1.5: Adhesion strength of the coating

Recently it has been shown that although the corrosion resistance increases with increasing Mg content, the adhesion strength of the coating simultaneously decreases. Therefore, it must be studied in more detail what causes this lack of adhesion strength in Zn coatings with high Mg content and what parameters influence this. This section will give an overview of the research conducted on this matter up until now.

1.5.1: Cause of loss of adhesion strength

First of all, it must be understood why the addition of Mg in the Zn coating leads to a decrease in adhesion strength. This mainly relates to the microstructural evolutions occur by the addition of Mg. As can be seen in Fig. 1.7 the phases that are present in the ZnMg coating change with increasing Mg content. At low Mg content, the coating mainly consists of pure Zn in addition to small additions of Mg_2Zn_{11}. Until at some point, around 7 wt.% Mg, the pure Zn disappears and is replaced by the formation of $MgZn_2$. The coating then exists of these two phases, until it reaches about 15 wt.% Mg, whereafter the coating will solely consist of $MgZn_2$ [14].

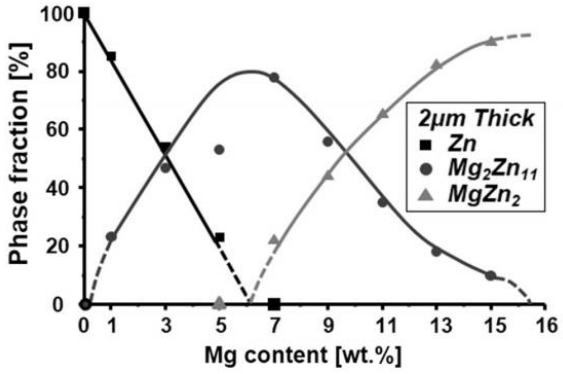

Fig. 1.7: Phase formation of ZnMg coating with increasing Mg content [14]

The decreased adhesion strength is directly related to the mechanical properties of the different phases and thus changes with increasing Mg content. Pure Zn is known as a soft and ductile phase, which is easy to plastically deform due to its low yield strength [14]. Opposed to this, the Mg_2Zn_{11} and $MgZn_2$ phases are both considered to be very brittle and have low strength. Therefore, they are not easily deformed and will break much faster than the pure Zn. Knowing this, it can be stated that the loss of adhesion strength is directly related to the decrease in pure Zn phase in the coating. At first, the coating consists of a Zn matrix containing islands of the Mg_2Zn_{11}. The Zn can make up for the brittleness of the intermetallic compound Mg_2Zn_{11}, and therefore the coating is

still able to bend properly and not delaminate. Beyond 7 wt.% Mg, the coating consists of a Mg_2Zn_{11} matrix including some islands of $MgZn_2$ and becomes too brittle to bend properly and the coating delaminates from the substrate. The research of Jung et al. [14] concluded that the portion of Mg in the coating was best to be kept under 6 wt.% to ensure proper adhesion strength, but still make use of the increased corrosion resistance.

The decrease of adhesion strength is not solely caused by the formation of the brittle intermetallic compounds Mg_2Zn_{11} and $MgZn_2$, but can also be explained by the work of adhesion present when Mg is added to the coating. Work of adhesion is referred to as the amount of work necessary to separate the coating from the steel substrate [15]. Fig. 1.8 shows how Mg performs compared to other elements regarding work of adhesion. From this it can be concluded that Mg has a lower work of adhesion than Zn, which means that it there is less work necessary to separate a coating containing Mg from the steel substrate than when it contains Zn. Thus this also yields the decreased adhesion strength of the coating when Mg content is increased.

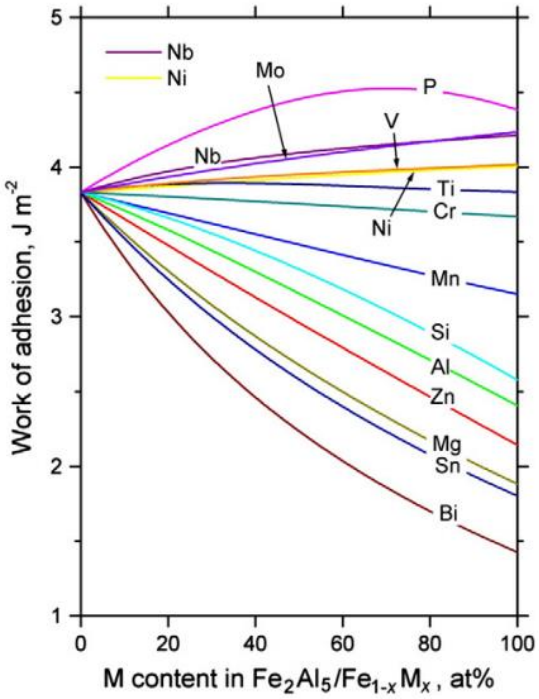

Fig. 1.8: Work of adhesion of different elements [36]

In the work of Sabooni et al. the adhesion strength of bi-layered ZnMg-Zn coatings, a coating consisting of a single layer of Zn on the substrate and a layer of ZnMg on top of that, was investigated and this also mentioned the work of adhesion. Here it was shown that the work of adhesion between the steel substrate and Zn layer was about 3 J/m², whilst that between the Zn layer and top ZnMg layer, constituting of the intermetallic compounds, was only around 1.6 J/m² [16], meaning that the Zn/ZnMg interface is inherently weaker compared to the steel/Zn interface.

1.5.2: Parameters influencing the adhesion strength of ZnMg coatings

Now that it is known what causes this loss of adhesion strength, it is also worthwhile to get an idea of what parameters possibly influence the adhesion strength next to the microstructural evolution and work of adhesion. As mentioned before, the research of Sabooni et al. [16] investigated the adhesion strength of bi-layered ZnMg-Zn coatings on a steel substrate with different Mg contents. In this research it was investigated which parameters could possibly influence the adhesion performance of the coating. In fig. 1.9 an overview is given of the four parameters that were found to influence adhesion: interfacial adhesion strength at the ZnMg/Zn interface, thickness of Zn interlayer (t_{Zn}), thickness of ZnMg top layer (t_{ZnMg}) and the interfacial defect density.

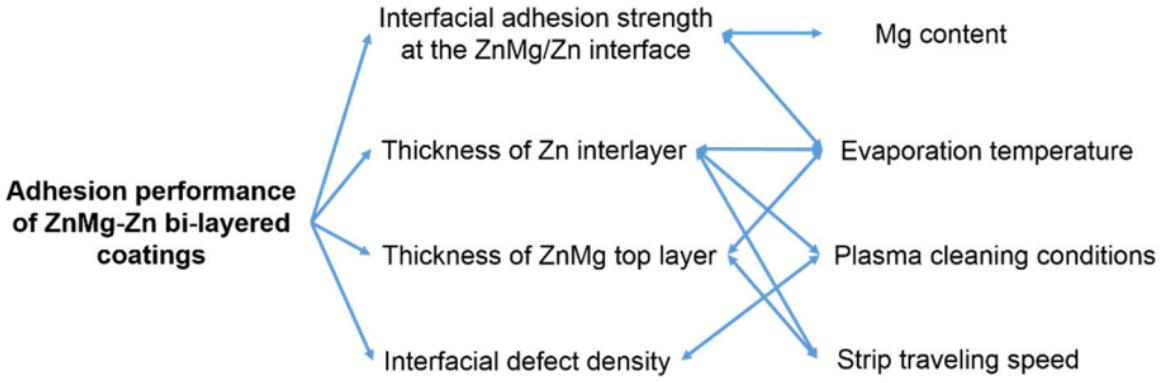

Fig. 1.9: Overview of interrelationships of parameters influencing the adhesion strength [16]

Each of these four parameters is also influenced by other specifications, which include the Mg content, evaporation temperature, plasma cleaning conditions and strip traveling speed. Down below it will be explained how these parameters are influenced by these specifications and how they can best be altered to obtain optimal adhesion strength at higher Mg content.

First of all, as stated before, the interfacial adhesion strength between the intermediate Zn layer and the top ZnMg layer have great influence on the adhesion performance of the coating. This adhesion strength is mainly influenced by the Mg content, which was explained in section 5.1, but is also influenced by the evaporation temperature.

Secondly, t_{Zn} also has an influence on the adhesion performance of the coating. This thickness does not influence the interfacial adhesion strength between the top and intermediate layer, as it was shown that this strength remains the same with increasing t_{Zn}, but it does help accommodate the stress and strain during bending. It was shown that there is a minimum t_{Zn} (=500 nm), which is necessary to pass the BMW crash adhesion test [16]. Therefore, the thickness of the intermediate Zn layer definitely has an influence.

Thirdly, the amount of defects present at the interface of the intermediate and top layer have a definite influence on the adhesion performance. Fig. 1.10 maps out the adhesion strengths of different coatings with different Mg contents, but also different defect densities at the Zn/ZnMg interface. Three groups were identified, ranging from no/low defects to numerous defects. It was shown through this research that coatings with similar Mg content could still yield different outcomes in the BMW crash adhesion test, if they had different amount of defects at the interface. Besides this, an exponential relationship between the adhesion strength and Mg content was also found for coatings containing no or few defects. It was noted that all coatings on this curve would pass the test, but if the coating would be too far below this it would fail.

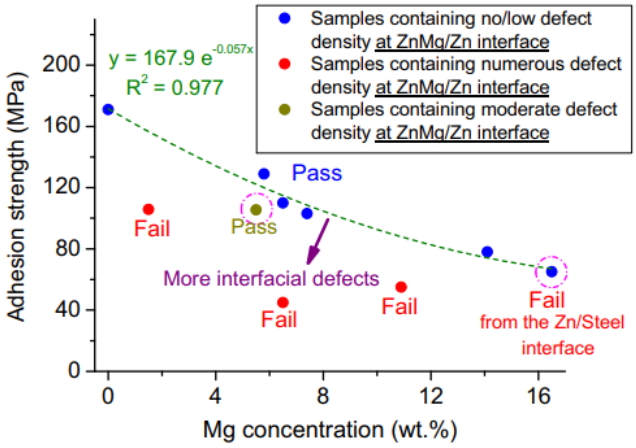

Fig. 1.10: Adhesion strength vs. Mg wt% in coatings with different interfacial defect densities [16]

Lastly, in contrast to t_{Zn}, t_{ZnMg} yields a maximum value instead of a minimum. The top layer of the coating can have a maximum value of 3.5 µm, which can slightly decrease with increasing Mg content (Sabooni et al., 2020). This decrease in the thickness of the ZnMg layer is caused by a decrease in ductility when Mg content is increased. Fig. 14 shows a simulation of the ZnMg-Zn coating in the BMW crash adhesion test. The coating in this simulation has a top layer of 6.8 µm, which is above the 3.5 µm and thus too thick. In fig. 1.11a it is shown that the top layer already starts to fail at a 45 degree angle, whilst the Zn layer is still in tact. Fig. 1.11b shows the final position of the coating. The coating is bend in a 90 degree angle, yielding large failures in the top layer whilst the Zn layer is still in tact due to its higher ductility.

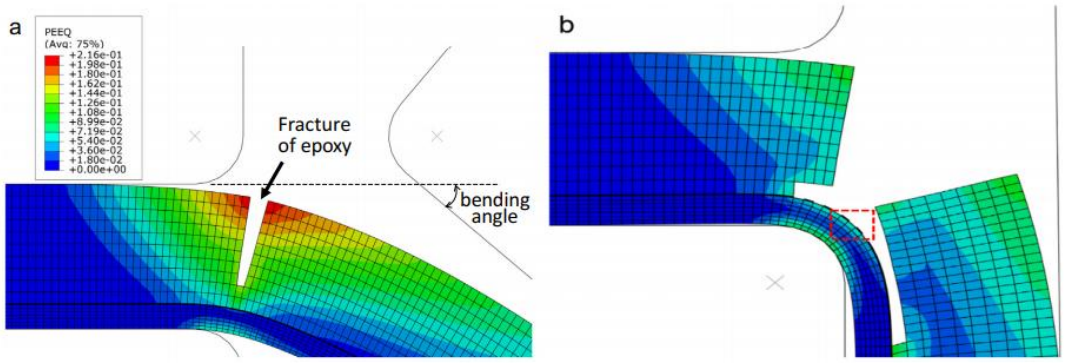

Fig. 1.11: Simulation of a ZnMg-Zn coating with a 6.8 µm top layer in the BMW adhesion test showing failure and plastic deformation [16]

2. Production techniques of Zn and Zn alloyed coatings

Currently, there are two main deposition techniques that are commonly used: electrodeposition and hot dip galvanizing. Hot dip galvanizing is also used by TATA Steel, who is the problem owner in this specific research. Recently, a new deposition technique has come up, called physical vapor deposition, which shows great advantages over traditional techniques and is also better fitted for coatings with higher Mg content. This section will give an overview of the three previously named techniques, their advantages and disadvantages and why physical vapor deposition is chosen as the appropriate techniques for the coatings with higher Mg contents.

2.1: Electrodeposition

The first deposition technique, electrodeposition, is based on the same kind of principle of an anode and cathode which is also present in the corrosion of steel explained in section 1. In this technique an anode, cathode, external circuit and plating solution are used [17]. An overview of the principle on which the electrochemical deposition technique is based is given in fig. 2.1.

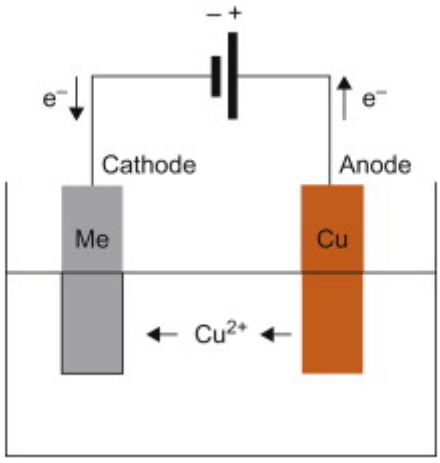

Fig. 2.1: Overview of the electrodeposition technique with which a coating can be applied to a steel substrate [18]

The anode is made up of the metal with which the steel substrate is supposed to be coated. The cathode is the steel substrate which requires coating. At the anode an oxidation reactions take place with which metal ions (of the coating metal) and electrons are released. The electrons travel through the external circuit towards the cathode. Meanwhile, reduction occurs at the cathode, where ions from the anode (or from the electrolyte solution in which both the cathode and anode are immersed) reduce to atoms by gaining electrons from the cathode which traveled there from the anode [17]. A protective coating slowly starts to form by means of this oxidation and

reduction. A great advantage of electrodeposition is that it is able to produce a wide variation in thicknesses (1µm – 1 mm), which is mainly dependent on the time the steel substrate is immersed in the solution [17].

Although the control of thickness is very important for coating application, especially in the automotive industry where it is demanded to have a coating as thin as possible, there are also many drawbacks to this technique. The main disadvantage of this technique has to do with the formation of hydrogen at the cathode. A great part of the current that is transported from the anode to the cathode is used to form hydrogen, which then disappears into the atmosphere, electrolyte solution or diffuses into the steel substrate [17]. This causes both a highly inefficient use of the current present and possible hydrogen embrittlement of the coating, which means that the coating becomes less ductile and strong which is disadvantageous for its application. Hydrogen embrittlement can be partly eliminated by post baking of the substrate, but this is not always sufficient.

A second drawback of electrodeposition is that it is not possible to use all types of metals as the anodic coating. For example, metals such as aluminum and magnesium are too active and have too small of an electrochemical potential range. If the potential present is outside of this range, all of the current present will be used for the formation of hydrogen [17]. As stated before, both aluminum and magnesium have shown to greatly improve the corrosion resistance of the coating and therefore this technique might not be the most appropriate for the advanced coatings which will be implemented in the future.

A third and last drawback of electrodeposition is that it uses very toxic solutions, as these yield a high and good deposition rate of the coating. A lot of water has to be used to make up for this toxicity, and therefore this technique is not the very environmentally friendly.

2.2: Hot Dip Galvanizing

Hot Dip Galvanizing (HDG) is one of the most commercially applied techniques due to its economic value [17]. In fig. 2.2 an overview is given of what a regular continuous HDG process looks like. The main step of HDG is the immersion of the steel substrate in a bath of the molten metal from which the coating is supposed to be made up of, in this example the zinc bath in the bottom right corner of the figure [3]. Although this is the main step, there are several necessary steps prior and post immersion in the metal bath. For example, beforehand the surface of the substrate has to be cleaned to remove any unwanted elements, where after a flux coating has to be applied to ensure that oxidation cannot take place on the cleaned substrate surface [17]. After cleaning, the substrate is put through a furnace to establish recrystallization, which is carried out at about 700 degrees. This temperature varies depending on the type of steel substrate

and also has to be increased when increasing line speed. When the substrate exists the furnace it is quickly cooled down to about 460 degrees, which is the approximate temperature of the metal bath in which it will be immersed. After immersion into the metal bath, the excess liquid metal is forced back into the bath and the substrate passes through the annealing furnace after which it is cooled and exits the process [3].

HDG has the advantage that it is a well-established economical process and that it can produce thick zinc coatings of high quality [17]. Although it is of good quality, the

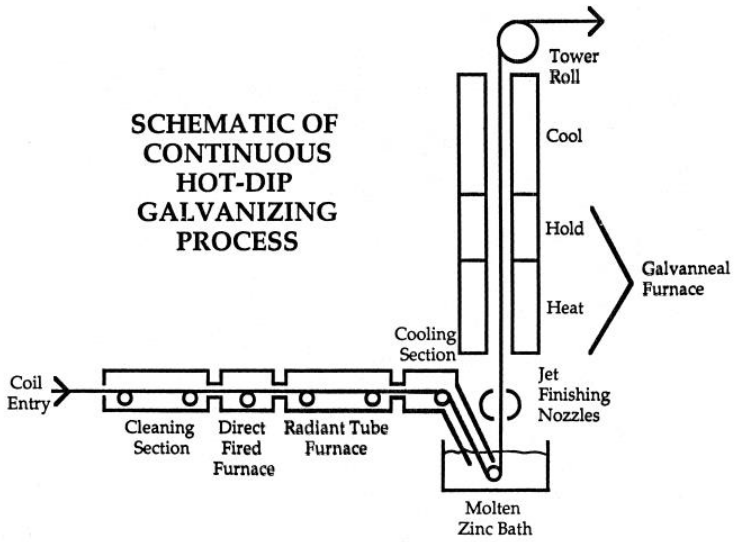

Fig. 2.2: Overview of the continues hot-dip galvanizing process for producing protective coatings on steel products [3]

thickness is not always equal which can be considered as quite an issue. Also, similar to electrodeposition, hydrogen embrittlement is also possible in HDG, making up another disadvantage of this technique.

Lastly, this technique is not applicable on the next generation of steels, such as advanced or high strength steels. These steels are alloyed with certain elements, which are isolated from the substrate in the furnace prior to the metal bath, leading to the formation of oxides on the surface of the substrate before application of the coating [19].

2.3: Physical Vapor Deposition (PVD)

There are several types of physical vapor deposition (PVD) processes, but they are all based on the same principle. Each of them consists of the same basic steps. First, the material, usually zinc or zinc alloy, that has to deposited as a coating on the steel substrate has to be vaporized. After that, the vapor travels from its entrance towards an area of low pressure at the substrate. Lastly, the vaporized material condenses to form a very thin type of film on the steel substrate [20]. With this technique coatings

with thicknesses of just a few nanometers can be formed, but it also possible to produce thicknesses comparable to those of the previous methods.

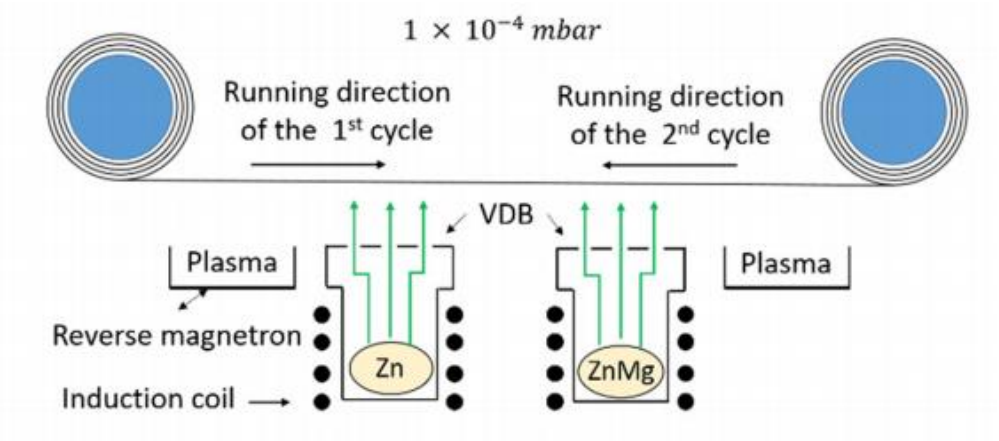

Fig. 2.3: Overview of a typical PVD process in which a protective coating is applied to steel substrate [16]

Physical vapor deposition is a novel technique compared to the HDG and electrodeposition. Another difference compared to the other two techniques is that PVD is a "dry" technique, whilst the others make use of a bath and are therefore "wet". This also comprises the first advantage of PVD: it is environmentally friendly, whilst traditional methods contribute significantly to environmental pollution [21]. As mentioned before, in electrodeposition, several toxic solutions are used and a lot of water is necessary to meet environmental regulations. In HDG very high temperatures are necessary to produce the melt bath (~ 460 °C – 700 °C), and therefore a lot of energy is necessary to facilitate this process and thus leaves a large ecological footprint. PVD does not make use of toxic solutions, nor does it require such high temperatures. The deposition temperature of this technique only reaches up to about 250 degrees [16].

Another advantage of PVD is that all types of inorganic and almost all organic materials can be applied onto the substrate as a coating. Also, it is possible to produce multi-layered coatings, which might be necessary, as will be explained in the next section which concerns the adhesion of the coating. Lastly, PVD can create coatings of only several nanometers and thus has great control over the coating thickness [16].

Although this technique seems to solve many problems that are currently experienced using the two traditional techniques, it also has some clear drawbacks. First of all, it was perceived that it is hard to coat complex shapes using this technique. Secondly, the technique carries great costs and is cannot yet produce nearly the same amount as traditional methods. Lastly, the process itself is more complex than that of the other techniques [20].

Even though these drawbacks are currently preventing the technique to be implemented in mass production, there are great prospects on solving this. In the paper by Navinšek et al. [22] it was shown that already some galvanic productions were replaced successfully by PVD variants. They also admit that it is necessary to make great improvements in continuous production PVD lines before they can meet current production levels and thus replace traditional techniques, but they do think this is possible and should be encouraged due to its many advantages.

2.4: Summary of the advantage of PVD technique for production of Zn and Zn alloyed coatings

In the previous three sub-sections three different application techniques were discussed. Also, some of their advantages and disadvantages were laid out. Although the first two techniques, electrodeposition and HDG, are now more commercially applied, it can clearly be seen that the novel PVD has great advantages over each of these. The use of electrodeposition leads to too much pollution, due to its usage of toxic solutions, and therefore also carries great energy costs. Besides this, there is the risk of hydrogen embrittlement using this technique, which should not be ignored. Although HDG makes up a slightly better contestant than electrodeposition and is also already widely commercially applied, there are some clear drawbacks. HDG will not be able to handle all developments in the industry. As stated before, HDG is not applicable to the next generation of steels, which have preferable properties over traditional steels and should therefore be used in steel structures. Also, in section 4 it was discussed that highly alloyed Zn-Mg coatings are very promising and should therefore be more thoroughly investigated and possibly commercially applied. A problem that appears with this is that it is not possible to add high wt% of Mg to the Zn bath in HDG, only a few percent's can be added. Also, Al also must be added in addition to Mg, as otherwise dross will form [12]. Therefore, PVD must and will be used to further investigate highly alloyed Zn-Mg coatings.

3. Techniques to Evaluate Adhesion

As the ZnMg coatings shows loss of adhesion, more research must be carried out to understand what causes this loss. When investigating what influence certain parameters have, different techniques can be used to measure the adhesion of the coating. In the past these techniques were mainly qualitative, but recently quantitative techniques which give a numerical indication of the adhesion have also been developed. This section will discuss some of the most commonly used techniques.

3.1: Peel-off test

The first techniques which will be discussed is the peel(-off) test. When such a test is carried out on a substrate with a coating, the goal is to fully separate the coating from the substrate by peeling it off. There are a lot of variations of the peel-off test, but the basic principle of it is shown in fig. 3.1. In this test the crack between the coating and substrate propagates as fast as the peeling speed and the force that is required to peel the coating off the substrate is recorded [23]. Using the force measured a force versus displacement figure can be constructed, from which the surface energy can be obtained.

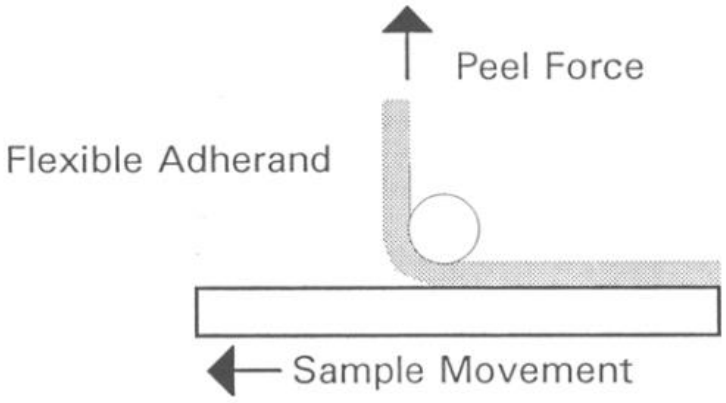

Fig. 3.1: Basic principle of the peel-off test which measures adhesion at the substrate-coating interface [23]

3.2: Indentation Debonding Test

The indentation debonding test an indenter is used, either Vickers or Brase, to apply a load on the coating applied to the substrate. When a certain load is reached, a lateral crack will start to form at the interface of the coating and substrate [24]. Several indentations will be made using different loads and the size of the lateral crack they yield will be recorded. If the crack does not form at the interface, but in either the substrate or the coating, it can be stated that the strength at the interface at least equal to that of the weak component in which the crack has propogated.

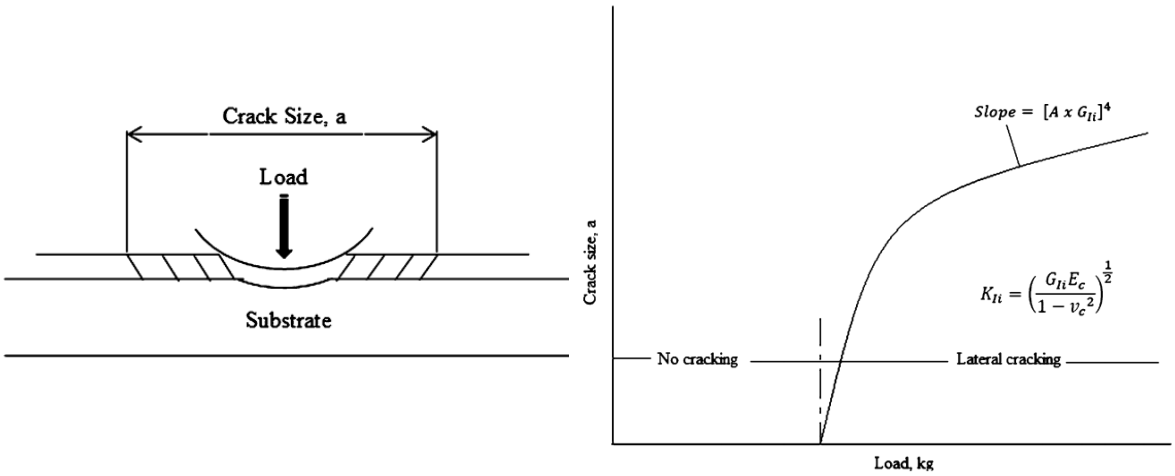

Fig. 3.2a: Overview of the Indentation debonding test measuring adhesion strength between substrate and coating; Fig. 3.2b: Relation between crack size and indentation load in the indentation debonding test [25]

A schematic overview of the indentation debonding test is given in fig. 3.2a. Using the different measurements of the crack size, a relation between load and crack size can be found, as shown in fig. 3.2b. From this graph the interfacial fracture toughness (K_{Ii}) can be found by using the two formulas shown in the graph, where E_c and v_c are the Young's modulus and Poisson's ratio of the coating and A is a constant [24].

3.3: Laser Spallation Test

In the laser spallation test a laser is used to induce spallation at the substrate-coating interface to measure adhesion. In this technique a pulsing laser, usually a YAG laser, is used to produce a laser impulse. This goes through a lens and then passes through a confining layer, as shown in fig. 3.3. Once passed through the confining layer it reaches an energy absorbing film, which is usually made up of gold or aluminum This film absorbs the energy provided by the layer and starts to expand, which produces a compressive stress aimed at the substrate and coating. Once the stress hits the free side of the coating, the one that is not attached to the substrate, a tensile stress will form which will occur in a backwards direction. After which the tensile stress reaches the substrate-coating stress, at which it can provide spallation of the substrate and coating if the tensile stress is higher than the interfacial strength. The interfacial strength can be computed using the stress which initiates spallation [26].

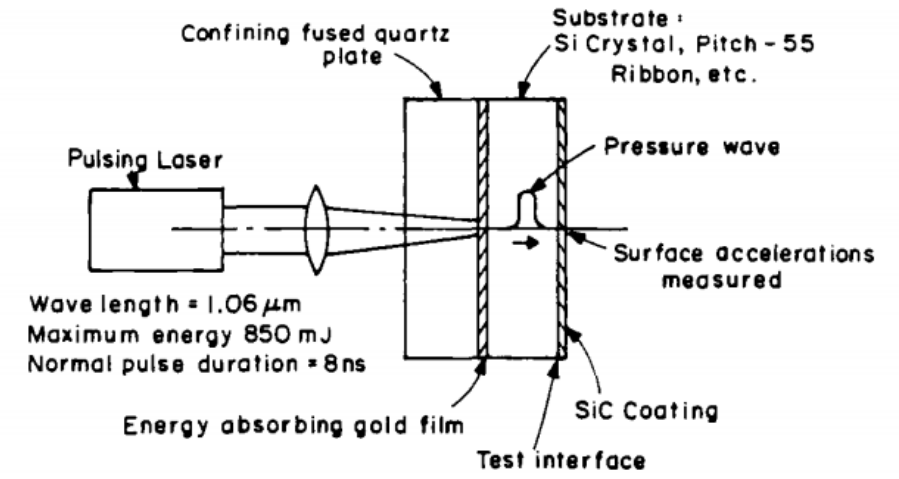

Fig. 3.3: Overview of the laser-induced spallation technique which measures adhesion at the substrate-coating interface [26]

3.4: Scratch Test

In a scratch test a diamond stylus is drawn across the surface of the coating on top of the substrate, as shown in Fig. 3.4. This stylus exerts a defined load and is drawn across a specific distance at constant velocity [25]. The load can be constant, gradually or incrementally increasing, but this depends upon the type of scratch test. Due to the force applied on the surface area a compressive stress which can cause two types of failures. Lateral cracking and lifting can occur, which is referred to as buckling, or the coating and substrate can be completely separated from each other, called spallation. The load at which the first failure at the substrate-coating interface starts to occur is called the critical load (L_c) [16]. This first failure can be detected using several techniques, including optical or scanning electron microscopy, acoustic emission and frictional force measurement. Which technique is used depends on the thickness of the coating, the first two are more appropriate for realistic thick coatings, whilst the latter is used for very thin (< 1 μm) coatings [24].

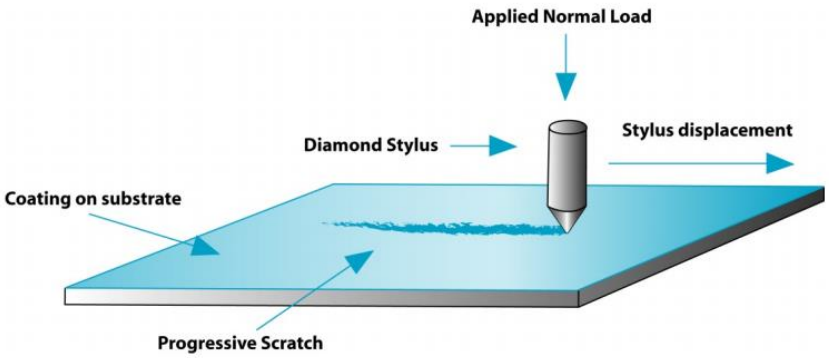

Fig. 3.4: Schematic overview of the scratch test technique measuring adhesion at the substrate-coating interface [35]

4. Materials and Methods

This section elaborates on the materials and methods used to obtain the necessary data for the analysis of the effect of Mg concentration on the different aspects. Firstly, it will be explained how the coatings are prepared using PVD, whereafter a more detailed explanation will be given of the different techniques used to obtain data concerning each aspect. Besides this, it will be stated how each of these techniques were used for this specific research.

4.1: Preparation of the coating using PVD

Single layer pure Zn and bi-layered ZnMg-Zn coatings with different Mg concentrations were produced using physical vapor deposition. The process that occurs in PVD was already introduced in section 4.3, but will be further elaborated on in this section. Before the coating can be applied, the substrate is pre-treated which removes surface oxides. This improves the adhesion of coating to the substrate by preventing the formation of interfacial defects. After the substrate is pre-treated, it is heated up, whereafter it can enter the PVD chamber. This chamber contains two crucibles, containing molten pure Zn and ZnMg, as was shown in Fig. 2.3. The materials inside the crucibles are then thermally vaporized using the induction coils, after which they pass through the vapor distribution boxes and deposit on the running steel strip. Using this technique, both single-layer pure Zn coatings and bi-layered ZnMg-Zn coatings can be produced. Bi-layered ZnMg-Zn coatings with different Mg concentration can be made by changing the Mg concentration in the ZnMg crucible.

4.2: Characterization techniques

In this section the different techniques used to obtain data on each of the aspects will be discussed. These techniques include Scanning Electron Microscope (SEM), X-Ray diffraction, nanoindentation test, scratch test, the modified Benjamin-Weaver model and polarization test. An explanation of each of these will be given.

4.2.1: Scanning Electron Microscope (SEM)

SEM is used to generate a clear microscopic image of the microstructure the coatings. This is done by releasing a beam of electrons, which is focused on a small spot of the material. This beam of electrons can be emitted by an electron gun, as shown in Fig. 4.1. The beam is then compressed by several lenses so that it focuses on a specific spot. The electron detector detects the signals that come from the scanned sample, which are formed by the interaction between the electrons and the material surface. These

signals then form into an image which gives information about the microstructure of the material scanned [27].

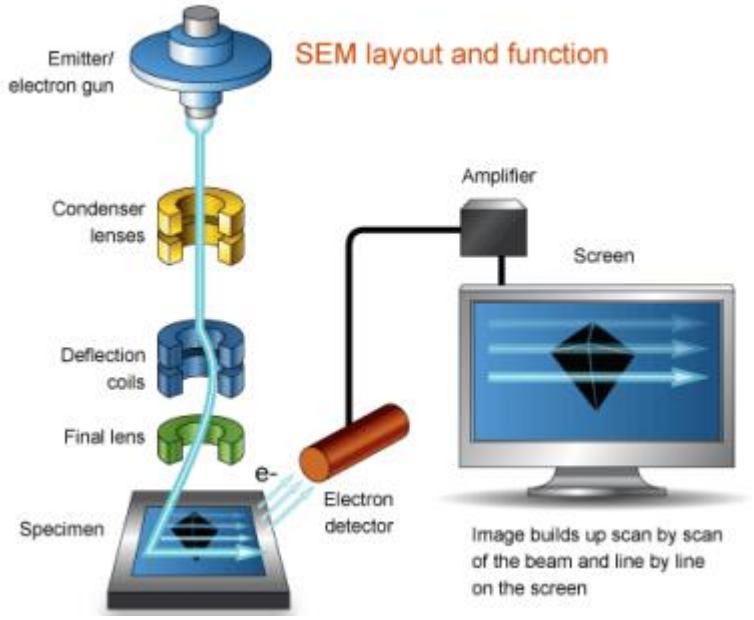

Fig. 4.1: Overview of the Scanning Electron Microscope Technique (SEM) used for analyzing the microstructure of a material [27]

4.2.2: X-Ray diffraction

X-Ray diffraction was used in the present investigation to study the structure and phase content, of the ZnMg-Zn coatings [28]. This information is retrieved by aiming a beam of scattered X-Rays at specific angles from different lattice planes in the material which produce XRD peaks. The pattern of these XRD peaks determine give an indication of how the atoms in the material are arranged.

4.2.3: Nanoindentation test

The nanoindentation test is based on the same principle as a regular indentation test, with which the hardness of a material can be determined. In such a test an indenter, which is hard and has a specific shape, is pushed into the tested material for a certain amount of time, after which its unloaded. The hardness of the material can then be

determined using the indentation load and the displacement depth of the material The nanoindentation test is based on the same principle as a regular indentation test, with which the hardness of a material can be determined. In such a test an indenter, which is hard and has a specific shape, is pushed into the tested material for a certain amount of time, after which its unloaded. The hardness of the material can then be determined

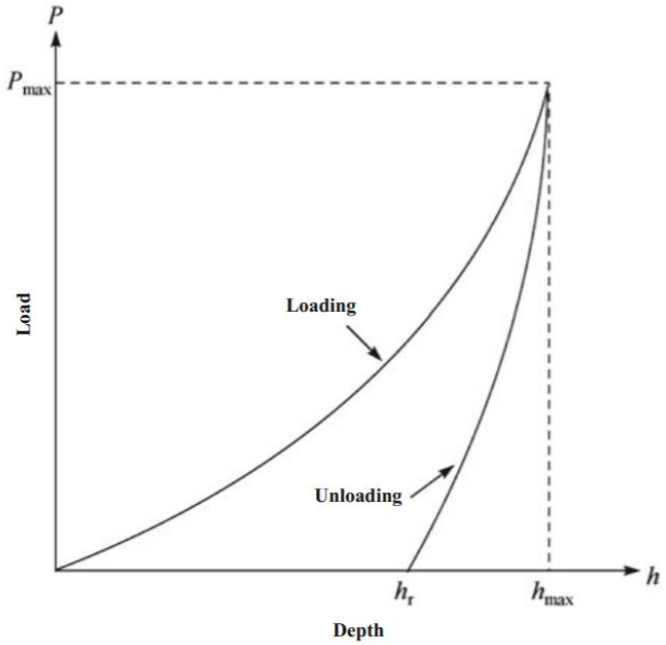

Fig. 3.2: Typical load-displacement curve obtained from a nanoindentation test [28]

using the indentation load and the displacement/area of the material [29].

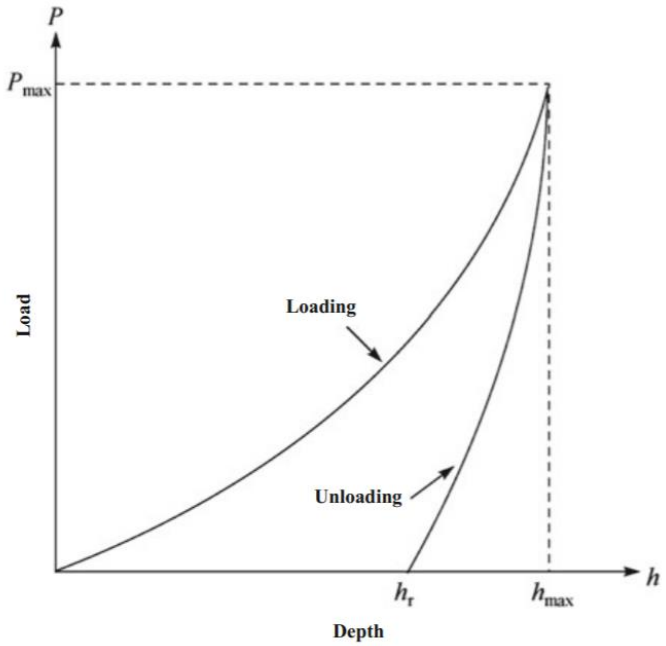

Fig. 4.2: Typical load-displacement curve obtained from a nanoindentation test [29]

In a nanoindentation test not just the hardness of the material can be determined, but also its elastic modulus, or other mechanical properties, such as viscoelasticity, toughness and strain-hardening effect. Using the load-displacement data obtained from the test a load-displacement curve is constructed. An example of such a curve is shown in Fig. 4.2. The loading curve is initiated by elastic deformation, which is characterized by the linear portion of the curve. When increasing the indentation load, plastic deformation emerges and the curve becomes non-linear. Once the indentation is finished and unloading starts, the elastic part of the deformation is recovered, whilst the permanent plastic deformation leaves the displacement which forms the indentation.

In this research, the nanoindentation test was used to determine the hardness and elastic modulus of the ZnMg coating. This can be computed using the following formula:

$$H = \frac{P_{max}}{A_c} \tag{4.1}$$

$$\frac{1}{E_r} = \frac{1 - v^2}{E} + \frac{1 - v_i^2}{E_i} \tag{4.2}$$

Where P_{max} is the maximum indentation load, A_c the projected contact area, v and E the Poisson's ratio and elastic modulus of the specimen, v_i and E_i the Poisson's ratio and elastic modulus of the indenter and E_r the effective elastic modulus [29].

4.2.4: Scratch test and modified Benjamin-Weaver model

The scratch test was already introduced earlier on in this report, but this sub-section will give a more thorough understanding of the technique and how it is used to obtain data concerning the substrate-coating adhesion.

In order to find a quantified value for the adhesion strength of the interface the Benjamin-Weaver model can be used, of which the equations are shown down below.

$$F = \frac{K\ a\ H}{\sqrt{R^2 - a^2}} \tag{4.3}$$

$$a = \left(\frac{L_c}{\pi\ H}\right)^{0.5} \tag{4.4}$$

In equation 4.3, F represents the adhesion strength in MPa, R is the radius of the tip of the indenter, K is a constant, H is the hardness of the substrate and a is expressed in equation 4.4. To compute the value of a the critical load obtained from the scratch test is used [16].

As this model was originally designed for the analysis of the adhesion strength of single coatings, the model should be adjusted to fit the bi-layered ZnMg-Zn coatings. The parameter that needs to be adjusted because of this extra layer is the substrate hardness, H. When there is only one coating layer present, this parameter is only dependent upon the hardness of the substrate, but due to the addition of the Zn interlayer, the hardness of this layer should also be taken into account when computing the adhesion strength at the ZnMg/Zn interface. Earlier on in this report it was shown that the ZnMg/Zn interface is weaker than the Steel/Zn interface and thus has a lower adhesion strength. Therefore, the critical load obtained from the scratch test is determined by the detachment of the ZnMg top layer, making the Zn interlayer part of the substrate [16]. Using the following equations, the substrate hardness can be determined:

$$\omega = \frac{thickness\ of\ zinc\ interlayer}{residual\ depth\ at\ L_c} \tag{4.5}$$

$$H_{composite} = \omega H_{Zn} + (1 - \omega) H_{steel} \tag{4.6}$$

In which the weight factor ω is determined using the thickness of the Zn interlayer and the residual depth at which the critical load was found. Thereafter the composite substrate hardness can be found using this weight factor and the hardness values of the Zn interlayer and substrate steel, as shown in formula 4.6.

4.2.5: Polarization test

A polarization test can be used to determine the corrosion rate of a coating. This technique is based on an electrochemical process, which is present in corrosion as explained in section 1.1. The test usually comprises of either two or three electrodes, where a small voltage is applied across two of these electrodes. After some time the flow of current between these two electrodes can be measured [30]. In this research, polarization tests were used to obtain the corrosion rate of pure Zn coatings exposed to different PVD chamber pressures, three ZnMg coatings with different Mg concentrations, two commercially applied coatings and a ZnMg11 coating exposed to deformation.

5. Results and Discussion

In this section a data analysis will be carried out with which the research questions can be answered. Four different aspects, microstructure and phase content, mechanical properties, substrate-coating adhesion and corrosion rate, will be examined in detail. The effect of Mg concentration on each of these aspects will be determined from which a final conclusion can be drawn about the range of Mg concentrations leading to the ZnMg coatings with the optimum quality.

5.1: Effect of Mg concentration on the microstructure and phase content of ZnMg coatings

When magnesium is added to the zinc coating the microstructure of the coating will obviously change and different intermetallic phases form. As microstructure can influence the properties of the coating, such as its mechanical properties and corrosion resistance, it is important to understand how the microstructure changes with increasing Mg concentration. Furthermore, it must be established whether the coatings contain interfacial defects, as these can also have a considerable influence on the mechanical properties and adhesion and therefore must be taken into account when drawing conclusions.

5.1.1: Microstructure of the ZnMg coating

To get an idea of how increasing Mg content influence the microstructure of the ZnMg coating, SEM were carried out of six coatings with different Mg contents (1.5, 3, 5.8, 7.4, 10.9 and 14 wt.% Mg) which are shown in Fig. 5.1 a-f. In each of the SEM micrographs the different layers (steel substrate, Zn interlayer and ZnMg top layer) can be clearly distinguished. It can be seen that some of the ZnMg top layers are consisted of different phases as different colors are recognized in the SEM micrographs.

It can be also concluded from Fig. 5.1 that some of the coatings (specially ZnMg1.5, ZnMg3 and ZnMg10.9) contains interfacial defects which is visible in black spots at the interface of ZnMg/Zn and/or Steel/Zn. The other three coatings (ZnMg 5.8, ZnMg 7.4 and ZnMg14) contain only few or no defects. The presence of interfacial defects in some of the coatings can influence on some of the coatings properties, for example on that of the critical load used for the computation of adhesion strength. As the defects make the coating less strong and thus diminish its quality, it is very likely that non-optimal results are obtained from coatings with defects. Therefore, it is very important to take these defects into account when drawing conclusions.

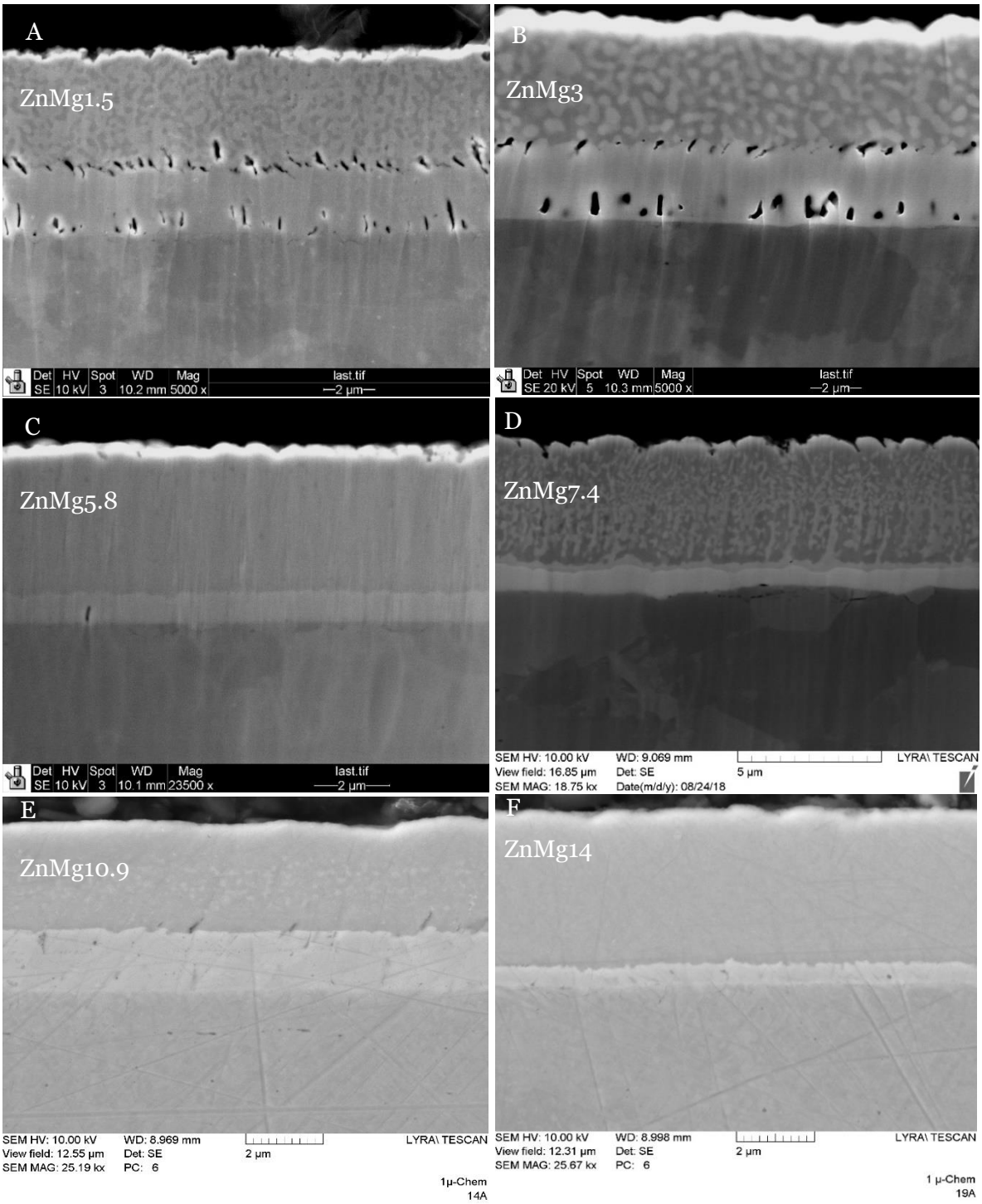

Fig. 5.1: SEM micrographs of the cross section of ZnMg-Zn coatings with different Mg concentrations; 1.5 wt.% (A), 3 wt.% (B), 5.8 wt.% (C), 7.4 wt.% (D), 11 wt.% (E) and 14 wt.% (F)

5.1.2: Phase content of the ZnMg coating

As discussed in the literature review, different intermetallic phases can form in the ZnMg coating depending on the Mg content. As seen in Fig. 5.2, when there is a low Mg content, the coating mainly consists of pure Zn phase combined with a low

percentage of Mg_2Zn_{11}. Once the Mg content is increased with a few percentages, the pure Zn phase starts to diminish, whilst the Mg_2Zn_{11} phase increases and becomes the major component of the coating. When 5.8 wt% Mg is reached the pure Zn phase has completely vanished, whilst another intermetallic phase, $MgZn_2$, slowly starts to form. As stated before, these intermetallic phases are both commonly known to be very hard and brittle, whilst pure Zn is more ductile, so this can definitely have an effect on the mechanical properties of the coating. When increasing the Mg content even more, above 5.8 wt%, the $MgZn_2$ phase content starts to grow and the Mg_2Zn_{11} phase slowly starts to diminish. Once 14 wt% Mg is reached the coating consists completely of $MgZn_2$. This phase formation is in accordance with previous researches, such as that of Jung et al. [14], although the Mg content at which certain phases disappear or start to form slightly differ.

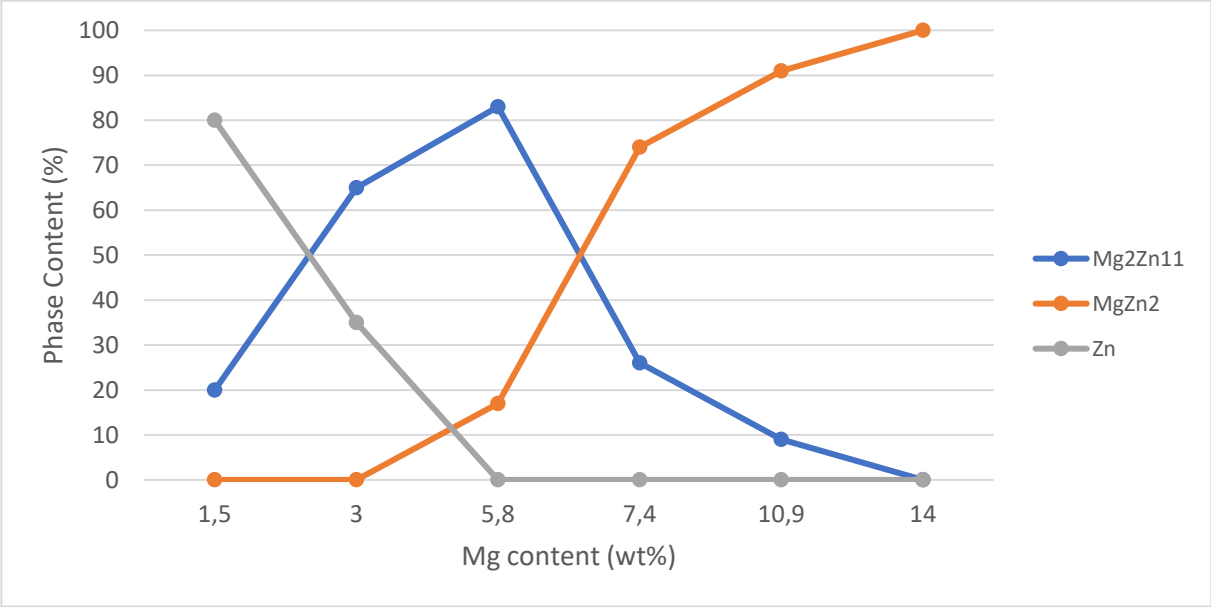

Fig. 5.2: The relation between magnesium concentrations and the phases contents present in PVD ZnMg coatings

5.2: Effect of Mg concentration on the mechanical properties of ZnMg coatings

The addition of Mg to the Zn coating also changes its mechanical properties, such as its hardness, elastic modulus and adhesion to the substrate. These mechanical properties are of great importance to the quality of the coating, as they can determine the durability of the coating in real applications. It is imperative that the steel can be bent into the desirable shape and that the coating remains properly attached to the substrate. Therefore, it is important to understand how these mechanical properties change with increasing Mg concentration and which Mg concentration range are optimum for further production.

5.2.1: Hardness and elastic modulus of the ZnMg coating

First of all, the hardness and elastic modulus for all of the coatings were measured. As Mg is added to the coating its microstructure and phase content changes, which influence the mechanical properties. In Fig. 5.3 the hardness of the coatings is shown, which shows an increasing trend. As mentioned in the previous section, the phases present in the ZnMg coating change with increasing Mg content. With low Mg content the coating mainly exists of ductile pure Zn phase and thus it is logical that the hardness is quite low at that point. When increasing the Mg content, more of the brittle Mg_2Zn_{11} phase starts to form and thus the hardness also starts to rise. From 6 wt% Mg on, it starts to increase with an even faster rate, because from that point on the coating consists solely of the two brittle intermetallic phases. It can be seen in the graph that the hardness starts to stabilize once ~ 8 wt% of Mg is reached, which can also be explained by the coatings phase content. Once higher Mg contents are added to the coating it mainly consists of the $MgZn_2$ phase and if 14 wt% is reached this is the only phase present. As the phase constitution does not change anymore from that point on, neither do its mechanical properties. It should also be mentioned that the ZnMg coating with 14% Mg shows a hardness of 5.2 GPa which is considerably higher than that of pure Zn (0.36 GPa).

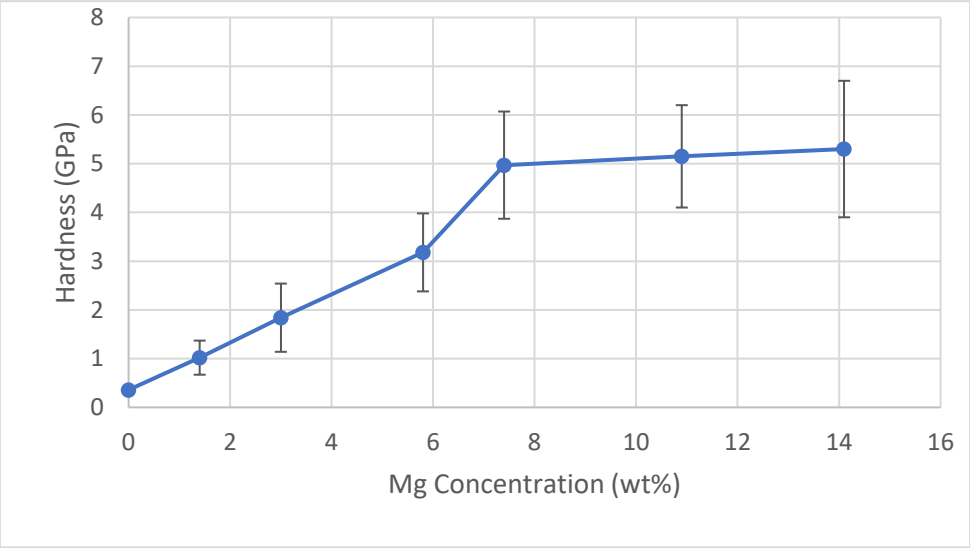

Fig. 5.3: Hardness of the ZnMg coating with increased Mg concentration

Looking at Fig. 5.4, it can be seen that the elastic modulus follows a trend similar to that of hardness. The elastic modulus defines the resistance to elastic deformation of the coating and thus coatings that are more stiff will yield a higher value. The elastic modulus of the pure Zn coating is ~ 55 GPa which increases to 104 GPa at Mg contents higher than 8%.

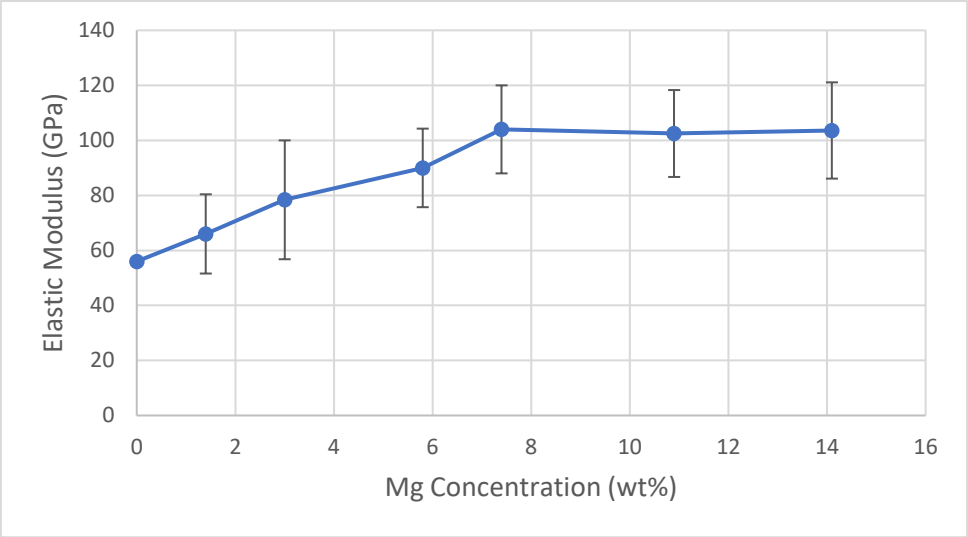

Fig. 5.4: Elastic modulus of the ZnMg coating versus Mg concentration

5.2.2: Resistance to plastic deformation of the ZnMg coatings

The values of hardness and elastic modulus of the coatings can be used to compute several ratios, which all give an indication of certain properties of the coating. Two of the most important ratios for coatings are the H/E and H^3/E^2 ratios [31]. The ratio that will be used in this research is the H^3/E^2 ratio, which gives an indication of the coatings resistance to plastic deformation [32]. As the coated steel will be further processed, for example when its used in the automotive industry, it is important that it can be bent into the right shape without cracking. Therefore, it is important to know whether the coating is still able to plastically deform with increasing Mg concentration.

As seen in Fig. 5.5, the resistance to plastic deformation shows a similar trend to that of hardness and elastic modulus. With low Mg content, there is barely any resistance to plastic deformation, but when the Mg content is increased this starts to increase slightly. Until 6 wt.% Mg it has only increased a little, but after this the curve becomes much steeper until it starts to stabilize after 8 wt.%. As it is favorable to have a low resistance to plastic deformation, lower Mg content seems to be preferable for this property.

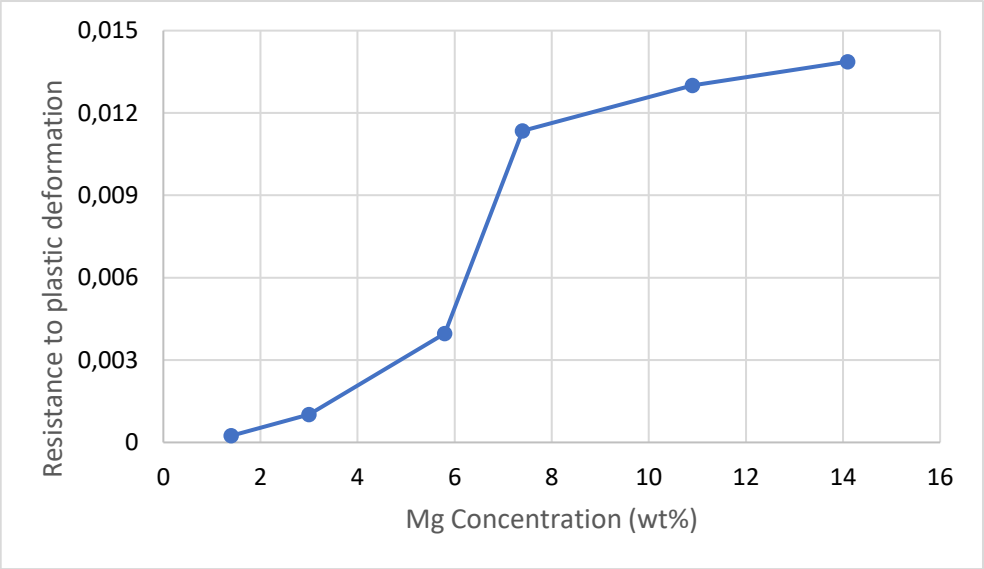

Fig. 5.5: Resistance to plastic deformation (H^3/E^2 ratio) of the ZnMg coating with increased Mg concentration

5.3: Effect of Mg concentration on the substrate-coating adhesion of ZnMg coatings

The next property of the ZnMg coating that will be examined is its adhesion to the underlying layer or steel substrate. In the literature review it was shown that this aspect is one of the main problems that arise with increased Mg concentration [14].

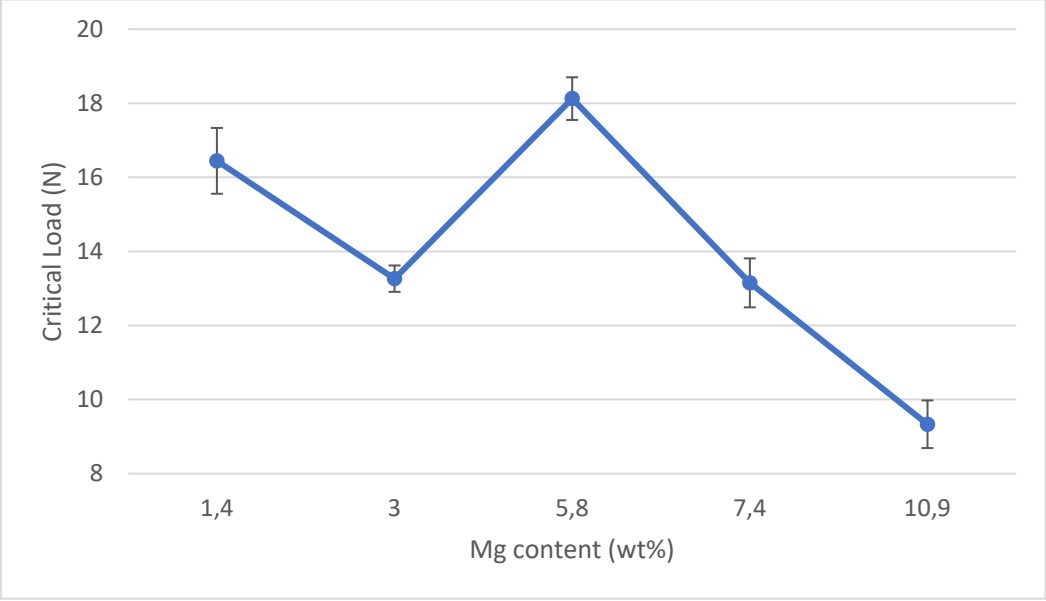

Fig. 5.6: Critical load obtained from scratch tests on ZnMg coatings with different Mg concentrations

A series of scratch tests were carried out on the coatings from which a critical load of delamination was obtained. This critical load is the load at which the adhesive failure is initiated in the coating. Although this critical load is yielded from the scratch test

which is supposed to say something about the adhesion of the coating to the substrate, no conclusions can be directly drawn from this parameter in our experiments. This is due to the fact that there are too many parameters of the coating-substrate system that influence the critical load. These parameters can be either intrinsic or extrinsic, meaning that they either have to do with the properties of the substrate or coating or the settings of the scratch test itself. The most important parameters are the substrate hardness, coating thickness, coating hardness, surface roughness, loading rate, indenter tip radius and friction between the indenter and the coating [33]. As some of these parameters differ for the coatings, it is hard to compare their adhesion using the measured critical load from the scratch tests. As seen in table 5.1 the thickness of the Zn interlayer and thus the coating thickness differs a lot over the investigated samples. Also, as shown in the previous sub-sections, the hardness and elastic modulus, and thus the H/E ratio, of the coatings also change with increased Mg concentration. Besides this, the first two coatings contain some interfacial defects and therefore these coatings will also yield a lower critical load in the scratch test compared to a defect-free coating with the same chemical composition. Therefore, no sound conclusions can be drawn from the critical load on its own.

As stated before, the critical load can be used in Benjamin-Weaver model which makes use of the following formulas [16]:

$$F = \frac{K\ a\ H}{\sqrt{R^2 - a^2}} \tag{5.1}$$

$$a = \left(\frac{L_c}{\pi\ H}\right)^{0.5} \tag{5.2}$$

Where F is the adhesion strength, K is a constant (0.2), H is the hardness of the substrate, R the radius of the tip of the indenter (200 µm) and L_c the critical load of delamination. As the investigated coatings consist of two layers of pure Zn and ZnMg, the model has to be adjusted slightly. The hardness of the substrate is not only dependent on that of the steel substrate, but also on the of the Zn interlayer, depending on the depth reached by the indenter at critical load. Therefore, the following formulas are used to compute a composite value for H: (5.3)

$$\omega = \frac{thickness\ of\ zinc\ interlayer}{residual\ depth\ at\ L_c}$$

$$H_{composite} = \omega H_{Zn} + (1 - \omega) H_{steel} \tag{5.4}$$

Table 5.1: overview of the different parameters used in the Benjamin-Weaver model, the computed adhesion strength and the results of the BMW adhesion test

Coating	Zn thickness (µm)	L_c (N)	Residual depth at L_c (µm)	ω (-)	$H_{composite}$ (GPa)	Adhesion Strength (MPa)	Results of BMW adhesion test
1.5 wt.% Mg	2.4	16.40	6.0	0.40	2.06	107.25	Fail
3 wt.% Mg	2.8	13.20	5.8	0.48	1.83	90.29	-
5.8 wt.% Mg	0.7	18.10	4.3	0.16	2.74	129.03	Pass
7.4 wt.% Mg	0.9	13.15	3.3	0.27	2.42	103.01	Pass
10.9 wt.% Mg	1.6	9.33	2.0	0.80	0.93	54.73	Fail
14.1 wt.% Mg	0.6	8.00	1.9	0.32	2.30	77.66	Pass

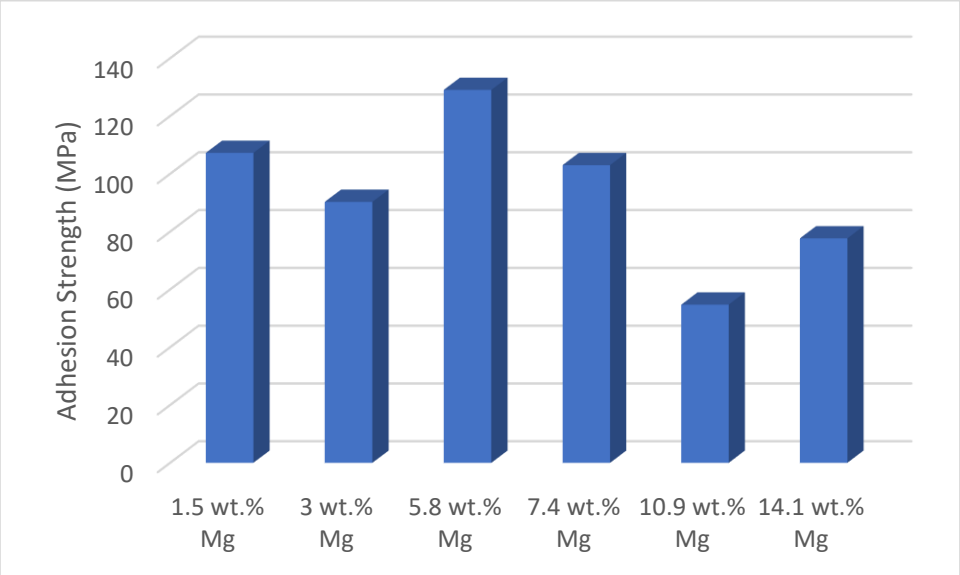

Fig. 5.7: Adhesion strength calculated using the modified Benjamin-Weaver model for the ZnMg-Zn bi-layered coatings containing different Mg concentrations

In table 5.1 different parameters used in the computation of the adhesion strength and the results of the BMW adhesion test are shown and in Fig. 5.7 the adhesion strength is depicted in a bar graph. When looking at Fig. 5.7, the adhesion strength seems to be very randomly distributed and not contain any trend, but the adhesion strength computed is dependent upon a lot of parameters which are not all the same for each of the coatings. For example, it was stated before that the two coatings with the lowest Mg content contain a lot of defects at both interfaces, which influences the critical load measured during the scratch test. This critical load is then used in the computation of the adhesion strength and therefore also changes this outcome.

In the literature review an overview was given of parameters that have an influence on the adhesion performance of the ZnMg coating, of which one was the defect density. In table 5.1 it can be seen that not all of the coatings passed the BMW adhesion test, including the one with the lowest Mg concentration. This is possibly caused by the high

porosity in this coating. Earlier in this report, a connection was found between the defect density of a coating and its results in the BMW adhesion test. Coatings with higher defect densities, such as the coatings with the lowest Mg content (1.5 wt.% Mg), were found to fail the bending test, whilst coatings with similar Mg content and no defects could pass the test. Therefore, the failure of the three coatings at the BMW adhesion test (1.5, 3 and 10.9 %) probably correlate to the defects present, which was shown in section 2.1.1., which also yielded lower adhesion strength.

If the three aforementioned coatings (1.5, 3 and 10.9 wt.% Mg) are disregarded, a trend starts to form in Fig. 5.7. The adhesion strength of the coating then clearly decreases with increased Mg concentration and therefore, regarding this aspect, a lower Mg concentration is more favorable.

5.4: Corrosion performance of the ZnMg coating

As discussed in the literature review, many previous researches have shown that ZnMg coatings yield better corrosion resistance than traditional coatings. Although they all agree that the addition of Mg has a positive effect on this aspect, the amount with which the corrosion rate is decreased and to what extent increase of Mg content has an effect on this differs a lot. This of course depends upon the atmosphere/test to which the coatings are exposed. For this research the corrosion rates of a few ZnMg coatings and two traditional coatings were obtained using a polarization test. Besides this, the effect of strain on the corrosion rate of the coating was also studied, as this also has to be taken into account for further processing of the coated steel.

5.4.1: Effect of PVD chamber pressure on corrosion rate

Another parameter that can possibly influence the corrosion rate of the coating is the deposition chamber pressure during the PVD process. It is important to test this as it costs a lot of energy, and thus money, to bring the pressure in the PVD chamber to such low levels. PVD is performed in a vacuum chamber, meaning that the pressure is very slim to non-existent. Although the pressure is thus already very low and changes in this are only minor, there seems to be a positive effect on corrosion rate when diminishing this pressure to an even smaller quantity. Four pure zinc coatings were produced using four quantities of chamber pressure (0.1, 0.01, 0.001 and 0.0001 mbar), where after their corrosion rates were established using a polarization test and microstructures were examined using SEM micrographs.

In Fig. 5.8 the SEM micrographs of the pure Zn coatings produced with different chamber pressures are shown. It can be clearly seen that the microstructure of the coating changes considerably with reduction of chamber pressure. At 0.1 mbar, the coating still contains a lot of pores that reach all the way from the top of the coating to

the coating-substrate interface, thus making it possible for corrosive elements in the atmosphere to penetrate the coating and corrode the steel substrate. With reduction of chamber pressure these pores take a different shape. They are still present, both at the top of the coating as well as on the substrate-coating interface, but they become smaller and do not reach through the entire coating thickness anymore. Therefore, it would be logical if the corrosion rate would decrease with this decrease in pores.

In Fig. 5.9 the corrosion rates of the different coatings are displayed in a bar chart. It can be clearly seen that the corrosion rate diminishes when lower chamber pressures are used during the production of coatings. When the pressure is reduced from 0.1 to 0.0001 mbar, thus means a thousand times smaller, the corrosion rate is almost two times as lower and thus the corrosion resistance is greatly improved. Although each of the measurements have a significant amount of standard deviation, it can be stated that even with this, taking into account the least favorable measurements, the corrosion rate is still clearly reduced with decreased pressure. Besides this, it can also be seen in Fig. 5.9 that similar corrosion performance compared to HDG can be reached using PVD with a 0.01 mbar pressure. With even lower pressures (e.g. 0.0001 mbar), the corrosion performance of the PVD produced coating is considerably better. Therefore, it can be stated that it is definitely useful to keep the PVD chamber pressure as low as possible, as it will then outperform the commercially applied HDG. When using this in the future production of ZnMg coatings, it might be wise to first investigate whether this parameter also has such a positive influence on that specific type of coating, as these results were generated from pure Zn coatings.

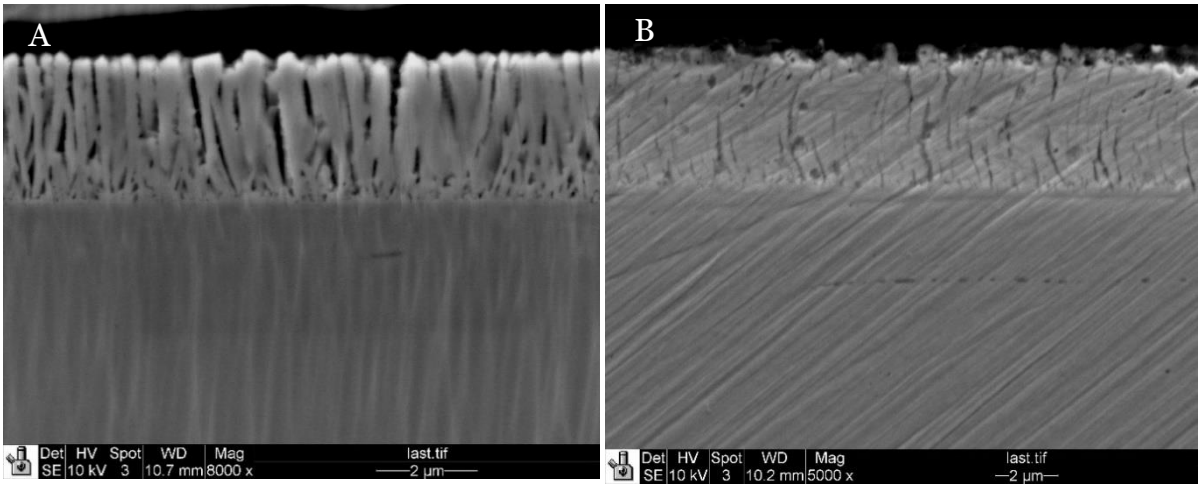

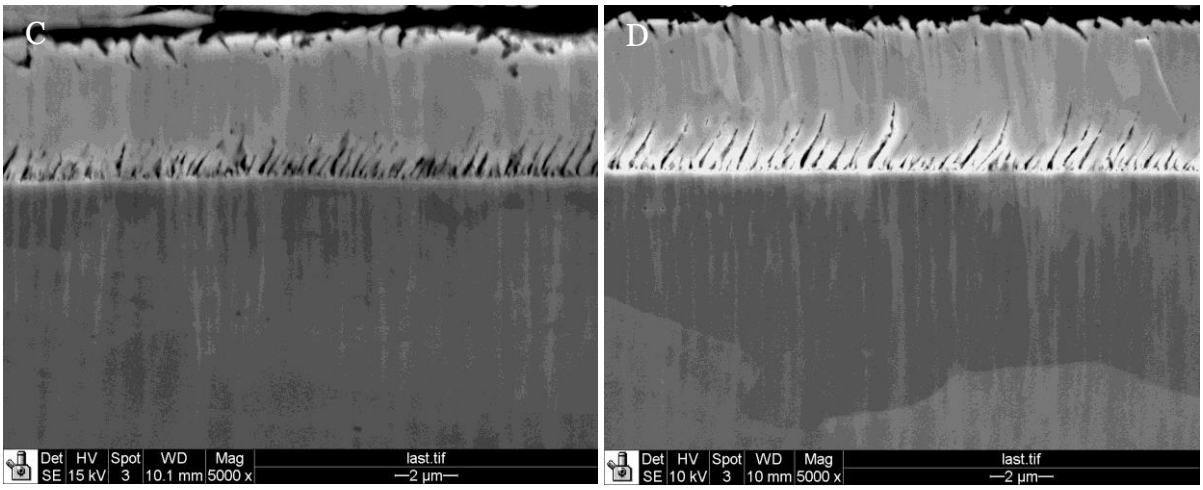

Fig. 5.8: SEM micrographs of pure Zn coatings produced at different PVD chamber pressures: 0.1 mbar (A), 0.01 mbar (B), 0.001 mbar (C) and 0.0001 mbar (D)

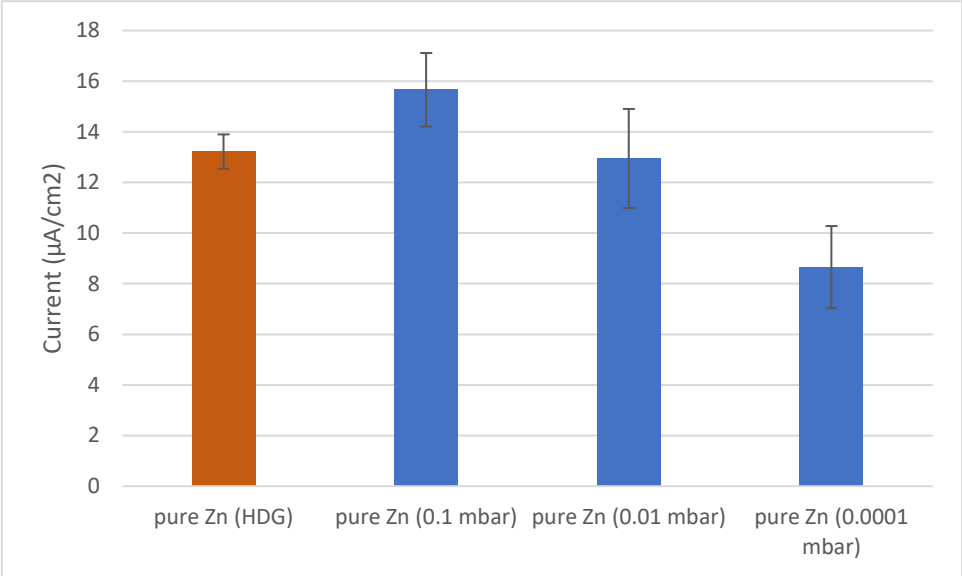

Fig. 5.9: Corrosion rates of pure Zn coatings produced at different PVD chamber pressures compared to the commercially applied HDG pure Zn coating

5.4.2: Corrosion rate of ZnMg coatings vs commercially applied coatings

Now that it is determined which PVD chamber pressure is most favorable for the corrosion rate of the coating, different ZnMg coatings can be tested for their corrosion resistance and compared to coatings that are currently being used as protective coatings for car body applications. As can be seen in Fig. 5.10 there is quite a decrease in corrosion rate and thus increase in corrosion resistance in ZnMg coatings with increasing the Mg content from 1.5 to 11% Mg. The corrosion rate of the PVD ZnMg coatings is at least about 6 times lower than that of a HDG pure Zn coating and 2 times lower than that of MagiZinc®. MagiZinc® is a novel protective coating, recently

developed by Tata steel, that consists of Zn with 1.8 wt% Mg and 1.8 wt% Al. As shown in the graph, even a small addition of Mg, only 1.5 wt%, already leads to a great increase in corrosion resistance. When increasing the Mg content, it can be stated that the corrosion rate decreases even more. Although the measurements have quite some standard deviation, it can still be stated that there is a decreasing trend when increasing the Mg content. Also, when looking at the difference in corrosion rate between the coatings with 1.5 and 6.5 wt% and 6.5 and 11 wt%, it can be stated that the decrease in corrosion rate possibly slows down with increasing Mg content and will most likely stabilize at a certain Mg concentration.

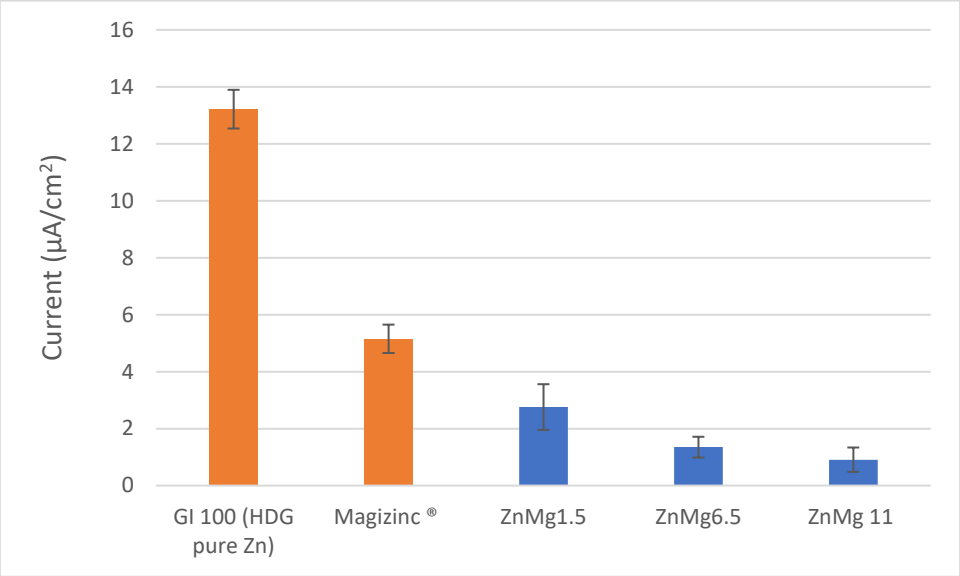

Fig. 5.10: Corrosion rates of three ZnMg coatings and two commercially applied coatings

5.4.3: Reason for improved corrosion performance

As it is now clear that the ZnMg coating performs much better concerning corrosion resistance than commercially applied coatings, it must be studied what causes this increase in performance. As mentioned before, the corrosion resistance of a coating can be influenced by the corrosions products formed on the coating when exposed to corrosive elements. To investigate what corrosion products are formed on ZnMg coatings that yield this improved performance, SEM micrographs were made, which are shown in Fig. 5.11. These SEM micrographs were made of three coatings: ZnMg1.5, ZnMg6.5 and MagiZinc®. As discussed before, one of the main corrosion products that yield protection for the steel substrate is the simonkolleite layer. When looking at the SEM micrographs in Fig. 5.11 it can be stated that the ZnMg coatings both contain simonkolleite, shown as nano flakes, whilst this is not clearly visible in the MagiZinc® coating. This explains why the corrosion rate of ZnMg coatings is much lower than that of MagiZinc®. Besides this, it can also be stated that an increase in Mg concentration leads to an even denser formation simonkolleite and thus to an even better protection and lower corrosion rate of the steel substrate. This can be seen by comparing the SEM

micrographs of the ZnMg1.5 and ZnMg6.5 coatings. The coating with 1.5 wt.% Mg already contains a lot of nano flakes showing the simonkolleite formed, but in the coating with 6.5 wt.% Mg these flakes are located even closer to each other filling up the gaps, yielding an even better corrosion resistance.

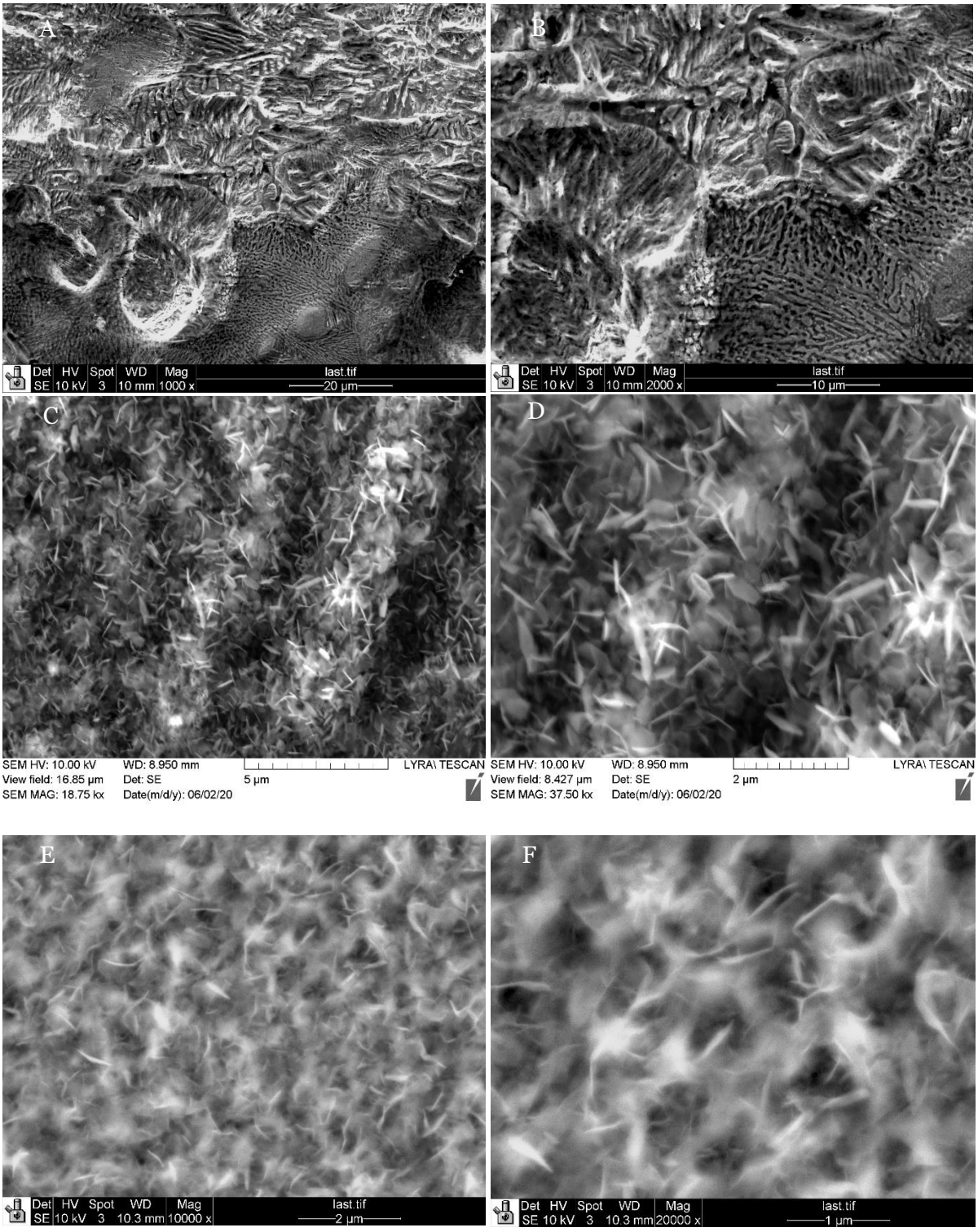

Fig. 5.11: SEM micrographs of the morphology of the corroded surface area of the MagiZinc® coating (A-B), ZnMg1.5 coating (C-D) and ZnMg6.5 coating (E-F)

5.4.4: Effect of deformation on the corrosion rate of ZnMg11-Zn coating

It is not only important to understand how the corrosion rate compares to other coatings, but it must also be known how this corrosion rate and the interfaces behave when the coating is deformed. When the coated steel is bent into the correct shape, it can be exposed to different amounts of strain. To examine the effect of deformation on the coating a uniaxial tensile test was carried out with three different amounts of strain (12.5%, 25% and 50%). In Fig. 5.12 SEM micrographs of the top surface and cross section of the coatings exposed to different amounts of strain are shown. From the top surface it can be seen that cracks are initiated at the strain of 12.5% and they propagate even more with further deformation. When looking at the cross sections of the deformed coatings, it can be examined how the different layers are effected by the strain to which they are exposed. It can be clearly seen that the ZnMg top layer is very brittle and therefore cracks very quickly when the strain exceeds ~ 2%, whilst the pure Zn interlayer just deforms and stretches out with increased strain. Also it can be seen that a crack starts to propagate along the ZnMg-Zn interface, showing that this interface is weaker than the interface of Zn/steel. It is in good correlation with the theoretical calculations of the work of adhesion where the work of adhesion at the ZnMg/Zn interface (1.6 J/m^2) is almost half of than that of the Zn/steel interface (3 J/m^2) [16].

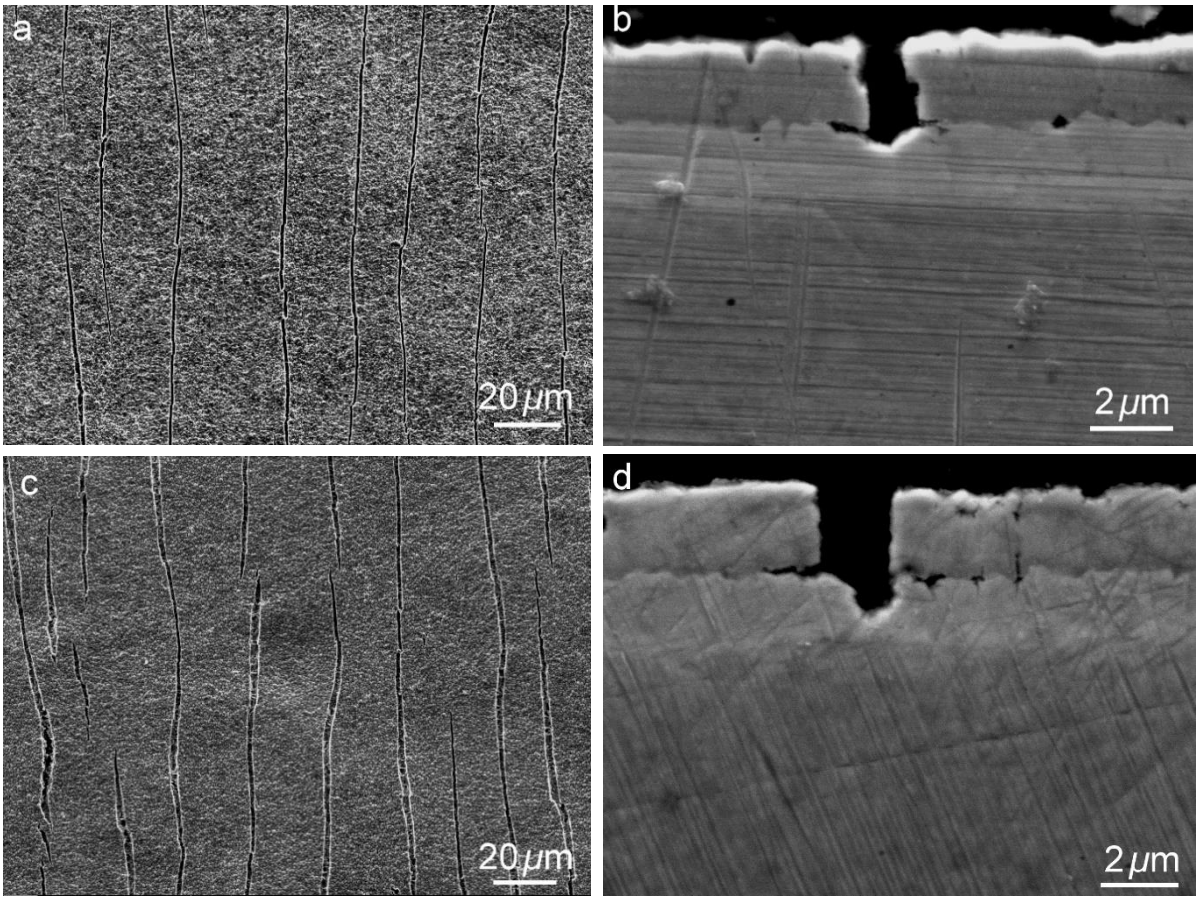

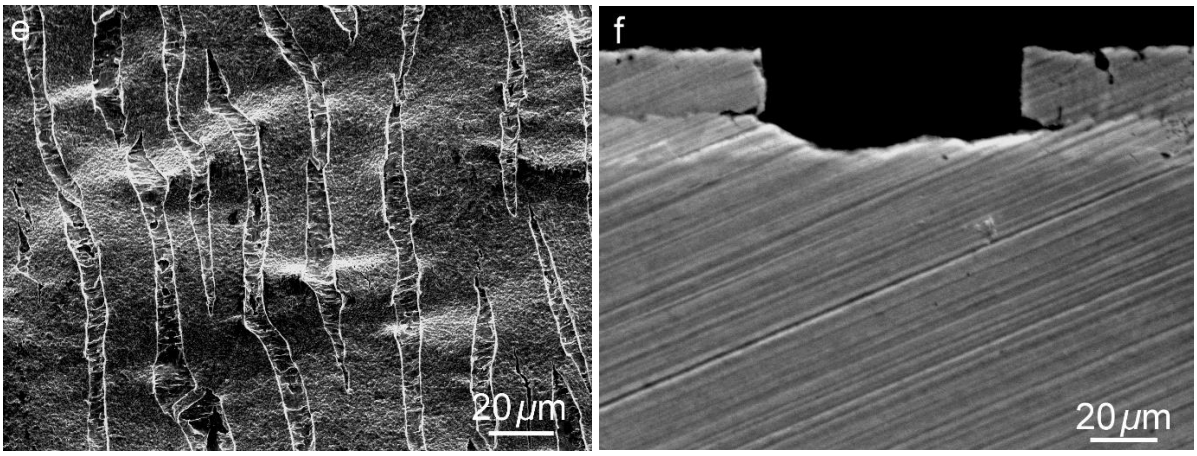

Fig. 5.12: SEM micrographs of the top surface and cross section of a ZnMg coating with 11 wt.% Mg exposed to three different levels of strain; 12.5% (a-b), 25% (c-d) and 50% (e-f)

Fig. 5.13 shows the corrosion current densities of the ZnMg11-Zn coating after they were exposed to different levels of strain. An increasing trend in the average corrosion rate of the coating appears when the strain is increased. Although the average of the corrosion rate measurements shown this trend, it is not completely reliable. As can be seen in the figure, each of the strain levels also have a certain standard deviation, which shows how much the measurements differ from each other. This standard deviation is especially a bit larger when 25% and 50% strain is applied to the coating. Therefore, the corrosion current density can differ quite a bit for those two levels of strain, but even taking this standard deviation into account, there is still a definite increase in corrosion rate, and thus diminished corrosion resistance, when a higher level of strain is applied to the coating. This means that the corrosion resistance will diminish if the coated steel is deformed in further processing. Although the corrosion resistance is diminished, even with 50% strain it is still much lower than that of Magizinc®, as seen in Fig. 5.13.

If in the future a ZnMg-Zn coating will be implemented into production, it might be wise to further investigate this effect of deformation on the corrosion rate for coatings with different Mg concentrations, as this was all based on a coating with 11 wt.% Mg.

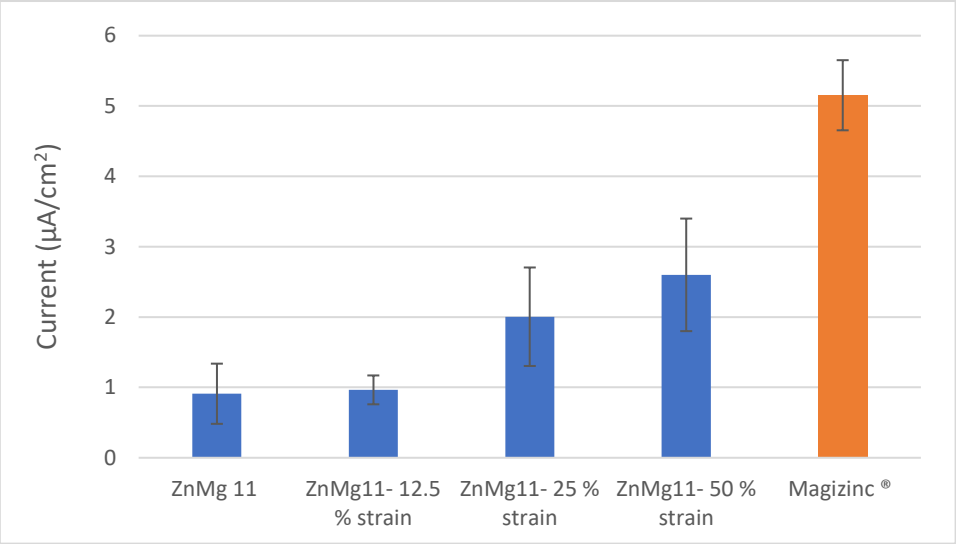

Fig. 5.13: Corrosion rates of ZnMg coatings with 11 wt% Mg exposed to different amounts of strain compared to the HDG MagiZinc® coating

5.5: Optimal Mg concentration for the ZnMg coating

Now that all four aspects, microstructure, mechanical properties, adhesion strength and corrosion resistance, have been thoroughly analyzed and discussed, a conclusion can be drawn about the optimal Mg concentration for the ZnMg coating. An indication will be given of the range in which this optimal Mg concentration lies, based on this research. However, before this coating can be implemented, more research has to be done, so it can be stated with certainty what the most favorable Mg concentration is.

From the results drawn in this section it can be stated that the optimal Mg concentration for some of the mentioned aspects contradict each other, therefore each of them should be considered carefully and a value should be found which is sufficient for each of these aspects. In section 5.1.2. it was found that the phase content of the ZnMg coating changes from the ductile pure Zn phase to hard and brittle intermetallic phases with increased Mg concentration, which has an effect on the mechanical properties of the coating. The hardness and elastic modulus, and thus the coatings resistance to plastic deformation, increase with increased Mg concentration and stabilize around 8 wt.% Mg. The values increase drastically and should be kept as low as possible. The increase in these values is the steepest between 6 and 8 wt.% Mg, therefore it would be wise to draw a line of the upper side of the range somewhere between 6 and 8 wt.%, as the hardness and elastic modulus of the coating are increased too much above these concentrations.

Secondly, considering the adhesion strength, it is also wise to pick a Mg concentration as low as possible, as this yields the best substrate-coating adhesion. Although it was also shown that the porosity, or defect density, of the coating also greatly influences the adhesion strength of the coating. This was shown by the coating with 14.1 wt.% Mg,

which still passed the BMW adhesion test as it contained very few to no pores. Therefore, if this porosity can be controlled, the Mg concentration can be made a little higher and still yield sufficient adhesion strength.

Lastly, the corrosion resistance of the coating should be taken into account. It was clearly shown that the corrosion resistance of the coating increases with increasing Mg concentration. Besides this, it was also seen that ZnMg coatings always outperform commercially applied pure Zn and MagiZinc® coatings, even with small Mg concentrations. The corrosion rate of the ZnMg coating decreases drastically going from 1.5 to 6.5 wt.% Mg, but after this the decrease becomes less visible. Therefore, the biggest improvement in corrosion performance is already gained with just a few percentages of Mg added and considering only the corrosion resistance, it does not necessarily make sense to add a very high wt.% Mg.

To sum this up, it can be stated that the optimal Mg concentration lies somewhere between 5 and 7 wt.% Mg, as this yields a much better corrosion performance, but still keep sufficient adhesion strength and resistance to plastic deformation.

6. Conclusion

In this research the effect of Mg concentration on the microstructure, mechanical properties, adhesion strength and corrosion resistance of the ZnMg coating was studied. The main conclusions drawn from this research are:

- The ductile pure Zn phase vanishes once the Mg concentration is increased to 5.8 wt.% and is replaced by hard and brittle intermetallic ZnMg phases ($MgZn_2$ and Mg_2Zn_{11}).
- The hardness, elastic modulus and resistance to plastic deformation of the ZnMg coating increase considerably until around 8 wt.% Mg, with the steepest increase between 5.8 and 7.4 wt.%, after which they stabilize.
- The adhesion strength of the ZnMg coating calculated using the modified Benjamin-Weaver model shows a decreasing trend with increasing Mg concentration, but is expected to stabilize at higher Mg concentrations, and is greatly influenced by the porosity of the coating.
- PVD yields a similar corrosion rate as HDG with a chamber pressure of 0.01 mbar, but when this pressure is decreased to 0.0001 mbar PVD yields a corrosion rate which is about 35% lower than that of HDG.
- The ZnMg coatings outperform commercially applied pure Zn and MagiZinc® coatings regarding corrosion resistance due to the formation of simonkolleite, which becomes more dense with higher Mg concentration and thus yields an even better corrosion performance.
- Deformation of the ZnMg coating leads to the formation and opening of cracks at the ZnMg layer resulting a higher corrosion rate.
- The optimal Mg concentration for the PVD ZnMg coating, taking all aspects into account, can be introduced between 5 and 7 wt.% Mg.

References

[1] V. Cicek and B. Al-Numan, Corrosion chemistry, Hoboken, N.J.: Wiley, 2011.

[2] Cathwell, “What is corrosion,” 2019. [Online]. Available: https://cathwell.com/what-is-corrosion/. [Accessed 17 04 2020].

[3] A. Marder, “The metallurgy of zin-coated steel,” *Progress in Materials Science,* no. 45, pp. 191-271, 2000.

[4] O. Kubaschewski and T. Massalki, “Binary allor phase diagrams,” in *Metals Park*, 1986, p. 1128.

[5] C. Jordan and A. Marder, “Fe-Zn phase formation in interstitial-free hot-dip galvanized at 450 degrees: Part I 0.00 wt% Al-Zn baths,” *Journal of Material Science,* no. 32, 1997.

[6] P. Pedeferri, Corrosion Science and Engineering, S.L.: Springer, 2019.

[7] N. Hosking, M. Ström, P. Shipway and C. Rudd, “Corrosion resistance of zinc-magnesium coated steel,” *Corrosion Science,* no. 49, pp. 3669-3695, 2007.

[8] J. Hernández and M. Suárez, “Effect of Chemical Bath Composition on Microstructure and Corrosion Resistance of Zinc Coatings by Hot Dip: A Review,” *Ingenius,* no. 23, pp. 40-52, 2020.

[9] M. P. Roman and R. F. Lynch, “Current Automotive Applications for GALFAN Coated Steel,” *SAE Transactions,* no. 98, pp. 678 - 689, 1989.

[10] C. Yao, S. Tay, J. Yang, T. Zhu and W. Gao, “Hot Dipped Zn-Al-Mg-Cu Coating with Improved Mechanical and Anticorrosion Properties,” *Intenational Journal of Electrochemical Science,* no. 9, pp. 7083 - 7096, 2014.

[11] J. Tanaka, K. Ono, S. Hayashi, K. Ohsasa and T. Narita, “Effect of Mg and Si on the Microstructure and Corrosion Behavior of Zn-Al Hot Dip Coatings on Low Carbon Steel,” *ISIJ International,* no. 42, pp. 80 - 85, 2002.

[12] A. Vimalanandan, A. Bashir and M. Rohwerder, “Zn-Mg and Zn-Mg-Al alloys for improved corrosion protection of steel: Some new aspects,” *Materials and Corrosion,* no. 65, pp. 392 - 400, 2014.

[13] T. Prosek, D. Persson, J. Stoulil and D. Thierry, “Composition of corrosion products formed on Zn-Mg, Zn-Al and Zn-Al-Mg coatings in model atmospheric conditions,” *Corrosion Science,* no. 86, pp. 231 - 238, 2014.

[14] W. S. Jung, C. W. Lee, T. Y. Kim and B. C. De Cooman, “Mg Content Dependence of EML-PVD Zn-Mg Coating Adhesion on Steel Strip,” *Metallurgical and Materials Transactions,* vol. July, no. 47, pp. 4594 - 4605, 2016.

[15] S. Sabooni, E. Galinmoghaddam, H. Cao, R. Westerwaal, C. Zoestbergen, J. De Hosson and Y. Pei, “New Insight into the Loss of Adhesion of ZnMg-Zn Bi-Layered Coatings on Steel Substrates,” *Surface and Coatings Technology,* no. 370, pp. 35 - 43, 2020.

[16] S. Sabooni, M. Ahmadi, E. Galinmoghaddam, R. Westerwaal, C. Boelsma, E. Zoestbergen, G. Song and Y. Pei, “Fundamentals of the adhesion of physical vapor deposited ZnMg-Zn bilayer coatings to steel substrates,” *Materials & Design,* no. 190, p. 108560, 2020.

[17] P. Chung, J. Wang and Y. Durandet, “Deposition processes and properties of coatings on steel fasteners - a review,” *Friction,* no. 7, pp. 389-416, 2019.

[18] J. Zhang and K. Hoshino, “Chapter 2,” in *Molecular Sensors and Nanodevices: Principles, Designs and Applications in Biomedical Engineering*, Elsevier, 2014, pp. 43 - 101.

[19] S. Sabooni, E. Galinmoghaddam, M. Ahmadi, R. Westerwaal, J. van de Langkruis, E. Zoestbergen, J. De Hosson and Y. Pei, “Microstructure and adhesion strength quantification of PVD bi-layeres ZnMg-Zn coatings on DP800 steel,” *Surface and Coatings Technology,* no. 359, pp. 227 - 238, 2019.

[20] G. Faraji, H. S. Kim and H. T. Kashi, “Chapter 1 - Fundamentals of Severe Plastic Deformation,” in *Severe Plastic Deformation*, Elsevier, 2018, pp. 19-36.

[21] A. Salam, Nanocoatings and Ultra-thin Films: Technologies and Applications, Woodhead Publishing, 2011.

[22] B. Navinšek, P. Panjan and I. Milošev, “PVD coatings as an environmentally clean alternative to electroplating and electroless processes,” *Surface and Coatings Technology,* no. 116, pp. 476 - 487, 1999.

[23] M. Sexsmith and T. Troczynski, “Peel strength of thermal sprayed coatings,” *Journal of Thermal Spray Technology,* no. 5, pp. 196 - 206, 1996.

[24] D. Rickerby, “A review of the methods for measurement of coating-substrate adhesion,” *Surface and Coatings Technology,* no. 36, pp. 541 - 557, 1988.

[25] M. Othman, A. Bushroa and W. Abdullah, “Evaluation techniques and improvements of adhesion strength for TiN coating in tool applications: a review,” *Journal of Adhesion Science and Technology,* no. 29, pp. 569 - 591, 2015.

[26] V. Gupta and A. Argon, “Measurement of Interface Strength by Laser Pulse induced Spallation,” *Materials Science and Engineering,* no. 126, p. 188, 1990.

[27] A. Mohammed en A. Abdullah, „Scanning Electron Microscope: a Review,” pp. 77-85, 2018.

[28] R. Kohli and K. Mittal, Developments in Surface Contamination and Cleaning, Elsevier , 2019.

[29] H. Wang, L. Zhu en B. Xu, Residual stresses and nanoindentation testing of films and coatings, Singapore: Springer , 2019.

[30] C. Andrade and C. Alonso, “Test methods for on-site corrosion rate measurement of steel reinforcement in concrete by means of the polarization resistance method,” *Materials and Structures,* vol. 37, pp. 623-643, 2004.

[31] J. Musil, F. Kunc, H. Zeman and H. Poláková, “Relationships between hardness, Young's modulus and elastic recovery in hard nanocomposite coatings,” *Surface and Coatings Technology,* no. 154, pp. 304 - 313, 2002.

[32] M. Kabir, P. Munroe, Z. Zhou and Z. Xie, “Study of the structure, properties, scratch resistance and deformation behaviour of graded Cr-CrN-Cr(1-x)AlxN coatings,” *Ceramics International,* no. 44, pp. 11364 - 11373, 2018.

[33] J. Valli, “A review of adhesion test methods for thin hard coatings,” *Journal of Vacuum Science & Technology,* no. 4, pp. 3007 - 3014, 1998.

[34] B. Beake, A. Ogwu and T. Wagner, “Influence of experimental factors and film thickness on the measured critical load in the nanoscratch test,” *Materials Science and Engineering,* no. 423, pp. 70-73, 2006.

[35] P. Leroux, D. Li and A. Herrmann, “Industrial coating scratch and wear evolution,” Nanovea, 2014.

[36] G.-M. Song and W. G. Sloof, “Effect of Alloying Element Segregation on the Work of Adhesion of Metallica Coating on Metallic Substrate: Application to Zinc Coatings on Steel Substrates,” *Surface and Coatings Technology,* no. 205, pp. 4632 - 4639, 2011.